

# INTEGRATED PATH STABILITY SELECTION

OMAR MELIKECHI<sup>1</sup> AND JEFFREY W. MILLER<sup>1</sup>

**Publication notice.** This version of the paper has been peer-reviewed and published in the *Journal of the American Statistical Association*. See <https://doi.org/10.1080/01621459.2025.2525589>.

**ABSTRACT.** Stability selection is a popular method for improving feature selection algorithms. One of its key attributes is that it provides theoretical upper bounds on the expected number of false positives,  $E(\text{FP})$ , enabling false positive control in practice. However, stability selection often selects few features because existing bounds on  $E(\text{FP})$  are relatively loose. In this paper, we introduce a novel approach to stability selection based on integrating stability paths rather than maximizing over them. This yields upper bounds on  $E(\text{FP})$  that are much stronger than previous bounds, leading to significantly more true positives in practice for the same target  $E(\text{FP})$ . Furthermore, our method requires no more computation than the original stability selection algorithm. We demonstrate the method on simulations and real data from two cancer studies.

---

## 1. INTRODUCTION

---

Stability selection is a widely used method that uses subsampling to improve feature selection algorithms (Meinshausen and Bühlmann, 2010). It is attractive due to its generality, simplicity, and theoretical control on the expected number of false positives,  $E(\text{FP})$ , sometimes called the *per-family error rate*. Despite these favorable qualities, existing theory for stability selection—which heavily informs its implementation—provides relatively weak bounds on  $E(\text{FP})$ , resulting in a diminished number of true positives (Alexander and Lange, 2011; Hofner et al., 2015; Li et al., 2013; Wang et al., 2020). Stability selection also requires users to specify two of three parameters: the target  $E(\text{FP})$ , a selection threshold, and the expected number of selected features. Several works have shown that stability selection is sensitive to these choices, making it difficult to tune for good performance (Haury et al., 2012; Li et al., 2013; Wang et al., 2020; Zhou et al., 2013).

The limitations of stability selection are illustrated in Figure 1. Here, we simulate data  $y_i = \mathbf{x}_i^T \boldsymbol{\beta}^* + \epsilon_i$  for  $i \in \{1, \dots, n\}$ , where  $n = 200$  is the number of samples,  $p = 1000$  is the number of features, and  $(\mathbf{x}_1, y_1), \dots, (\mathbf{x}_n, y_n)$  are observations of  $n$  independent random vectors  $(\mathbf{X}_i, Y_i)$ , where  $\mathbf{X}_i \in \mathbb{R}^p$  and  $Y_i \in \mathbb{R}$ . The features and noise are generated as  $X_{ij} \sim \mathcal{N}(0, 1)$  independently, and  $\epsilon_i \sim \mathcal{N}(0, \sigma^2)$  independently given  $\mathbf{X}_1, \dots, \mathbf{X}_n$ , where  $\sigma^2 = \frac{1}{2n} \sum_{i=1}^n (\mathbf{x}_i^T \boldsymbol{\beta}^*)^2$  so that the empirical signal-to-noise ratio is 2. The coefficient vector  $\boldsymbol{\beta}^*$  has  $s = 20$  nonzero entries  $\beta_j^* \sim \text{Uniform}([-1, -0.5] \cup [0.5, 1])$ , located at randomly selected  $j \in \{1, \dots, p\}$ , and all other entries are 0. The results in Figure 1 are obtained by simulating 100 random data sets as above and running stability selection using lasso as the base estimator (Tibshirani, 1996). A selected feature is a *true positive* if its corresponding  $\boldsymbol{\beta}^*$  entry is nonzero, and is a *false positive* otherwise.

---

<sup>1</sup>DEPARTMENT OF BIOSTATISTICS, HARVARD T.H. CHAN SCHOOL OF PUBLIC HEALTH, BOSTON, MA

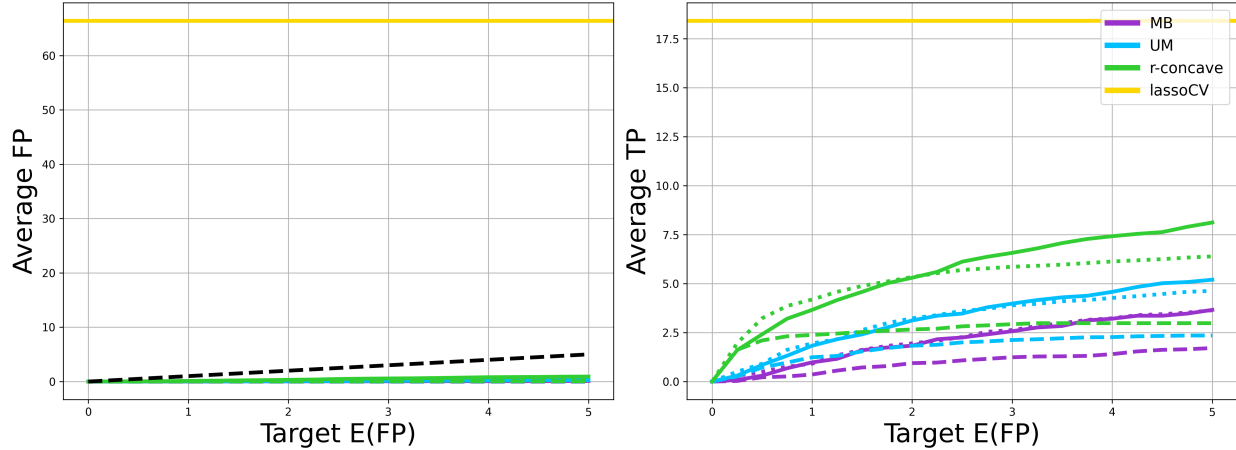


FIGURE 1. *Tradeoff between FP and TP.* Stability selection is overly conservative, yielding a small number of false positives (FP) at the expense of a small number of true positives (TP). Meanwhile, lasso has a high TP, but also a very high FP. (*Left*) Average FP versus target  $E(FP)$  for the original stability selection method of Meinshausen and Bühlmann (2010), denoted MB, and the unimodal (UM) and  $r$ -concave methods of Shah and Samworth (2013) at thresholds  $\tau = 0.6, 0.75$ , and  $0.9$  (solid, dotted, and dashed lines, respectively), as well as lasso with cross-validation, which does not depend on the horizontal axis. The black dashed line is the target  $E(FP)$ . (*Right*) Average TP versus target  $E(FP)$  for the same methods.

The horizontal axis in Figure 1 is the target  $E(FP)$ . The vertical axes show the actual numbers of false positives (FP) and true positives (TP), averaged over the 100 data sets. The stability selection methods have relatively few true positives on average, and usually 0 false positives, undershooting the target  $E(FP)$ . On the other hand, lasso with regularization parameter chosen by cross-validation (lassoCV) produces around 18 true positives, but over 65 false positives. This is a known trade-off: Typically, stability selection is too conservative, while lasso with cross-validation is not conservative enough (Alexander and Lange, 2011; Leng et al., 2006; Zou, 2006). Furthermore, while UM and  $r$ -concave outperform MB, both rely on additional assumptions and have less transparent bounds on  $E(FP)$ ; in particular,  $r$ -concave requires an additional algorithm to implement and its bound does not admit a closed form, making it difficult to interpret (Shah and Samworth, 2013).

In this article, we introduce *integrated path stability selection* (IPSS) to address these limitations. We prove that IPSS satisfies bounds on  $E(FP)$  that are orders of magnitude stronger than existing stability selection bounds, yielding more true positives for the same target  $E(FP)$ . This is a key advantage since the actual number of false positives is unknown in practice, so stronger bounds enable one to increase the true positive rate while maintaining control over  $E(FP)$ . IPSS is also simple to implement and requires no more computation than stability selection.

The rest of the article is organized as follows. In Section 2, we describe our setup, provide background on stability selection, and discuss related work. In Section 3, we introduce IPSS, and in Section 4, we present our theoretical results. Section 5 contains an extensive simulation study, and Section 6 contains applications of IPSS to prostate and colon cancer. Section 7 concludes with a discussion.

---

 2. STABILITY SELECTION AND PREVIOUS WORK
 

---

In this section, we define the setup of the problem (Section 2.1) and describe existing stability selection methods (Section 2.2) and other related work (Section 2.3).

**2.1. Setup.** Suppose  $S \subseteq \{1, \dots, p\}$  is an unknown subset to be estimated from observations  $\mathbf{z}_1, \dots, \mathbf{z}_n$  of  $n$  independent and identically distributed (iid) random vectors  $\mathbf{Z}_1, \dots, \mathbf{Z}_n$ . Let  $\hat{S}_\lambda(\mathbf{Z}_{1:n}) \subseteq \{1, \dots, p\}$  be an estimator of  $S$ , where  $\mathbf{Z}_{1:n} = (\mathbf{Z}_1, \dots, \mathbf{Z}_n)$  and  $\lambda > 0$  is a parameter, and let  $\hat{S}_\lambda(\mathbf{z}_{1:n})$  denote the corresponding estimate obtained from the observed data. We refer to  $\hat{S}_\lambda$  as the *base estimator*, and allow it to be a random function, such as a stochastic optimization algorithm. In regression, we have an observation  $\mathbf{z}_i = (\mathbf{x}_i, y_i)$  of each  $\mathbf{Z}_i = (\mathbf{X}_i, Y_i)$ , where  $\mathbf{x}_i \in \mathbb{R}^p$  is a vector of features and  $y_i \in \mathbb{R}$  is a response variable. A canonical base estimator in this setting is the lasso algorithm (Tibshirani, 1996), in which case  $\hat{S}_\lambda(\mathbf{z}_{1:n}) = \{j : \hat{\beta}_j(\lambda) \neq 0\}$  where

$$\hat{\beta}(\lambda) = \arg \min_{\boldsymbol{\beta} \in \mathbb{R}^p} \frac{1}{2} \sum_{i=1}^n (y_i - \mathbf{x}_i^\top \boldsymbol{\beta})^2 + \lambda \sum_{j=1}^p |\beta_j|. \quad (2.1)$$

We also consider the minimax concave penalty, MCP (Zhang, 2010), the smoothly clipped absolute deviation penalty, SCAD (Fan and Li, 2001), the adaptive lasso (Zou, 2006), and  $\ell_1$ -regularized logistic regression (Friedman et al., 2010); see Section S4 for details. In an unsupervised learning setting such as graphical lasso, we have  $\mathbf{Z}_i = \mathbf{X}_i \in \mathbb{R}^p$ , without a response variable (Friedman et al., 2008). Additional background on graphical lasso and other examples of base estimators amenable to stability selection can be found in Section 2 of Meinshausen and Bühlmann (2010).

For a given  $A \subseteq \{1, \dots, n\}$ , define  $\mathbf{Z}_A = (\mathbf{Z}_i : i \in A)$  and let  $\hat{S}_\lambda(\mathbf{Z}_A)$  denote the estimator computed using only the data in  $\mathbf{Z}_A$ . A key quantity is the probability that feature  $j$  is selected when using half of the data. We denote this *selection probability* by

$$\pi_j(\lambda) = \mathbb{P}(j \in \hat{S}_\lambda(\mathbf{Z}_{1:\lfloor n/2 \rfloor})). \quad (2.2)$$

Stability selection and IPSS employ estimators of  $\pi_j(\lambda)$ , called the *estimated selection probabilities*  $\hat{\pi}_j(\lambda)$ , computed by repeatedly applying a base estimator to random subsamples of the data (Algorithm 1). The resulting *stability paths*  $\lambda \mapsto \hat{\pi}_j(\lambda)$ , which will be important in what follows, are shown in Figure 2. Both  $\pi_j(\lambda)$  and  $\hat{\pi}_j(\lambda)$  depend on  $n$ , but  $n$  is suppressed from notation since it is always fixed in this work. Notably, all our results are non-asymptotic, applying to any  $n \geq 2$ .

---

**Algorithm 1** (Estimated selection probabilities)
 

---

**Input:** Data  $\mathbf{z}_1, \dots, \mathbf{z}_n$ , base estimator  $\hat{S}_\lambda$ , parameter grid  $\Lambda$ , number of iterations  $B$ .

1: **for**  $b = 1, \dots, B$  **do**  
 2:   Randomly select disjoint  $A_{2b-1}, A_{2b} \subseteq \{1, \dots, n\}$  with  $|A_{2b-1}| = |A_{2b}| = \lfloor n/2 \rfloor$ .  
 3:   **for**  $\lambda \in \Lambda$  **do**  
 4:     Evaluate  $\hat{S}_\lambda(\mathbf{z}_{A_{2b-1}})$  and  $\hat{S}_\lambda(\mathbf{z}_{A_{2b}})$ .  
 5:   **end for**  
 6: **end for**

**Output:** Estimated selection probabilities  $\hat{\pi}_j(\lambda) = \frac{1}{2B} \sum_{b=1}^{2B} \mathbb{1}(j \in \hat{S}_\lambda(\mathbf{z}_{A_b}))$ .

---

In Algorithm 1 and throughout this work,  $\mathbb{1}(\cdot)$  denotes the indicator function:  $\mathbb{1}(E) = 1$  if  $E$  is true and  $\mathbb{1}(E) = 0$  otherwise. Note that  $\hat{S}_\lambda$  is evaluated on both disjoint subsets,  $A_{2b-1}$  and  $A_{2b}$ , at each iteration of Algorithm 1. This technique of using complementary pairs of subsets was

introduced by Shah and Samworth (2013). By contrast, in the original stability selection algorithm of Meinshausen and Bühlmann (2010),  $\hat{S}_\lambda$  is applied to only one subset of size  $\lfloor n/2 \rfloor$  at each iteration. The difference in empirical performance between the two approaches is minimal, but this slight modification simplifies the assumptions needed for the theory (Shah and Samworth, 2013).

The choice of  $\lfloor n/2 \rfloor$  samples is required for the theory of stability selection to hold, both in this paper and in previous works. An alternative approach is to randomly select  $n$  samples with replacement in each of the  $B$  subsampling steps (Bach, 2008). However, this bootstrap approach only guarantees that  $S$  is recovered asymptotically in the special case where lasso is the base estimator. By contrast, stability selection and IPSS provide finite sample control of  $E(FP)$  for arbitrary base estimators. Shah and Samworth (2013) also observe that the selection probabilities computed by sampling with replacement are very similar to those computed using Algorithm 1, suggesting that stability selection and IPSS depend little on whether subsampling is implemented with or without replacement.

**2.2. Stability selection.** Once the  $\hat{\pi}_j$  values are computed, the set of features selected by stability selection (Meinshausen and Bühlmann, 2010; Shah and Samworth, 2013) is

$$\hat{S}_{SS} = \left\{ j : \max_{\lambda \in \Lambda} \hat{\pi}_j(\lambda) \geq \tau \right\} \quad (2.3)$$

where  $\Lambda = [\lambda_{\min}, \lambda_{\max}] \subseteq (0, \infty)$  is an interval defined below and  $\tau \in (0, 1)$  is a user-specified threshold. The upper endpoint  $\lambda_{\max}$  is inconsequential provided it is large enough that all features have small selection probability, which is easy to determine empirically. Choosing  $\lambda_{\min}$  is considerably more subtle, since many or even all features satisfy  $\hat{\pi}_j(\lambda) \geq \tau$  as  $\lambda \rightarrow 0$ . While there is no consensus on how to choose  $\lambda_{\min}$  (Li and Zhang, 2017; Zhou et al., 2013), a standard approach is to use theoretical upper bounds on  $E(FP)$  as follows.

The MB, UM, and  $r$ -concave versions of stability selection all satisfy theoretical upper bounds of the form  $E(FP) \leq \mathcal{B}(q, \tau)$ , where  $\mathcal{B}(q, \tau)$  is an expression that depends on the method (MB, UM, or  $r$ -concave), the average number of features selected over  $\Lambda$ ,  $q = E|\bigcup_{\lambda \in \Lambda} \hat{S}_\lambda(\mathbf{Z}_{1:\lfloor n/2 \rfloor})|$ , and the threshold,  $\tau$ ; see Section 4.3. To determine  $\lambda_{\min}$ , two of the following three quantities must be specified: (i) the target  $E(FP)$ , denoted  $E(FP)_*$ , (ii) the threshold,  $\tau$ , and (iii) the target number of features selected,  $q_*$ . The third quantity is then obtained by setting  $E(FP)_* = \mathcal{B}(q_*, \tau)$  and solving. Once  $q_*$  is determined,  $\lambda_{\min} = \sup \{ \lambda \in (0, \lambda_{\max}) : E|\bigcup_{\lambda' \in [\lambda, \lambda_{\max}]} \hat{S}_{\lambda'}(\mathbf{Z}_{1:\lfloor n/2 \rfloor})| \geq q_* \}$  is empirically estimated and  $\Lambda = [\lambda_{\min}, \lambda_{\max}]$  is used in Equation 2.3.

The above construction elucidates some of the shortcomings of stability selection and motivates our formulation of IPSS. First, the inequalities  $E(FP) \leq \mathcal{B}(q, \tau)$  are replaced by equalities in order to determine  $\lambda_{\min}$  in a way that controls FP. Thus, while the recommended procedure does typically keep the actual FP smaller than  $E(FP)_*$ , it may be much smaller, as shown in Figures 1 and 3. This overconservative tendency leads to a lower TP than necessary. More precisely, weak bounds on  $E(FP)$  lead to large values of  $\lambda_{\min}$ , which prevent true features from being selected because their stability paths have not yet distinguished themselves from the noise (Figure 2). Second,  $E(FP)_*$ ,  $q_*$ , and  $\tau$  are interdependent, making it difficult to select these parameters in practice. Meinshausen and Bühlmann (2010) recommended taking  $\tau \in [0.6, 0.9]$ , but stability selection is sensitive to  $\tau$  even when restricted to this interval (Li et al., 2013; Wang et al., 2020). Nevertheless,  $\tau$  must be specified in most cases because one usually has little *a priori* knowledge to inform the choice of  $q_*$ . Finally, while one can in principle use a smaller  $\lambda_{\min}$ , it is unclear what value to choose and doing so would invalidate the  $E(FP)$  control guarantee, making it hard to interpret the results.

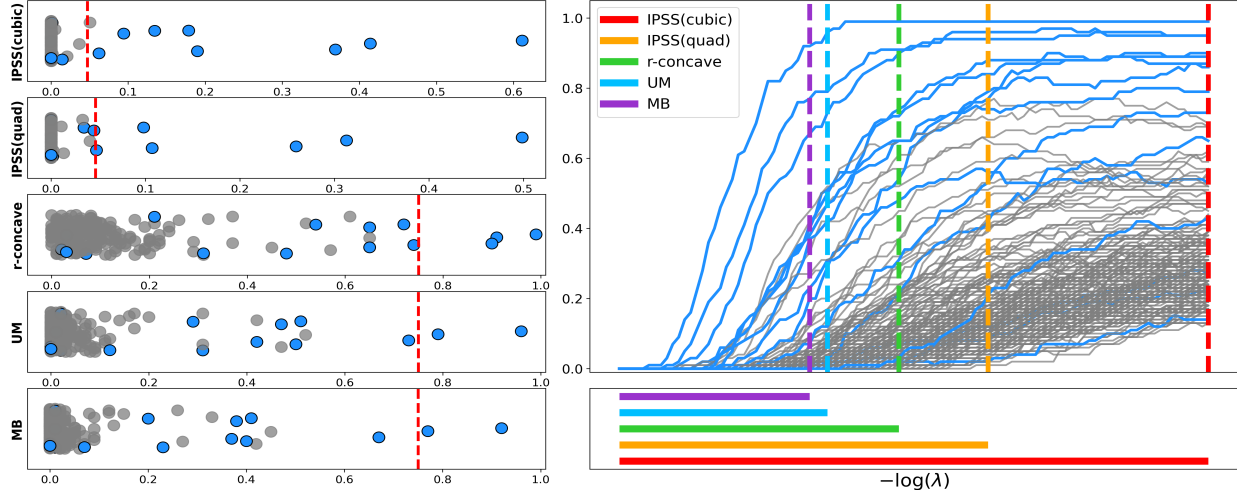


FIGURE 2. Linear regression with independent design as in Section 1 with  $n = 150$ ,  $p = 200$ ,  $\text{SNR} = 1$ , and  $s = 15$  true features. (Left) The horizontal axis is the score for each feature  $j$ , that is,  $\int_{\Lambda} f(\hat{\pi}_j(\lambda))\mu(d\lambda)$  for IPSS and  $\max_{\lambda \in \Lambda} \hat{\pi}_j(\lambda)$  for the others. The vertical axis is random jitter for visualization. True features are shown in blue, and red vertical lines show the threshold  $\tau$  separating selected and unselected features for each method. We use  $E(\text{FP})_* = 1$  for all methods, and for stability selection, we use  $\tau = 0.75$ . MB, UM,  $r$ -concave, IPSS(quad), and IPSS(cubic) identify 2, 2, 3, 6, and 8 true positives, respectively. All methods have 0 false positives except IPSS(cubic), which has 1, agreeing with the target  $E(\text{FP})$ . (Right) Estimated stability paths  $\hat{\pi}_j(\lambda)$ . Vertical dashed lines show  $-\log(\lambda_{\min})$  and horizontal lines below the plot show the intervals  $[-\log(\lambda_{\max}), -\log(\lambda_{\min})]$  for each method.

**2.3. Related work.** Stability selection was introduced by Meinshausen and Bühlmann (2010) and refined by Shah and Samworth (2013). These remain the preeminent works on stability selection and are the most commonly implemented versions to date. Zhou et al. (2013) provide the only other work we are aware of that aims to improve the selection criterion in Equation 2.3 and the  $E(\text{FP})$  bound. They propose *top- $k$  stability selection*, which averages over the  $k$  largest selection probabilities for each feature. The special case of  $k = 1$  is stability selection. While Zhou et al. (2013) provide theory for top- $k$  stability selection, their improvement upon the  $E(\text{FP})$  upper bound of Meinshausen and Bühlmann (2010) is considerably weaker than the improved bound provided by IPSS; compare Zhou et al. (2013, Theorem 3.1) to our Theorem 4.1. Moreover, introducing  $k$  increases the number of parameters, and results are sensitive to the choice of  $k$  (Zhou et al., 2013).

It is far more common for stability selection to be modified on an *ad hoc* basis to mitigate its sensitivity to parameters and overly conservative results. An example is the TIGRESS method of Haury et al. (2012), which uses stability selection to infer gene regulatory networks. To reduce sensitivity to the stability selection parameters, they use a selection criterion that averages over selection probabilities. It turns out that this is the special case of IPSS with  $f(x) = x$  (the function  $w_1$  in Section S3), whose analysis is relegated to the supplement because its bound on  $E(\text{FP})$  is not nearly as strong as those in Theorems 4.1 and 4.2. Another example is in the work of Maddu et al. (2022), where stability selection is used to learn differential equations. There the authors use a selection criterion based only on selection probabilities at the smallest regularization parameter. Finally, a common approach is to combine stability selection with other methods. Examples include

stability selection with boosting (Hofner et al., 2015) and grouping features prior to applying stability selection, which has been done in genome-wide association studies (Alexander and Lange, 2011). IPSS can be used instead of stability selection in such methods at no additional cost.

---

### 3. INTEGRATED PATH STABILITY SELECTION

---

In this section, we introduce IPSS (Section 3.1) and describe its parameters (Section 3.2), computational details (Section 3.3), and how it can be used to control the false discovery rate (Section 3.4).

**3.1. The IPSS criterion.** IPSS uses the same selection probabilities,  $\hat{\pi}_j$ , as stability selection. Once these are computed using Algorithm 1, the set of features selected by IPSS is

$$\hat{S}_{\text{IPSS},f} = \left\{ j : \int_{\Lambda} f(\hat{\pi}_j(\lambda)) \mu(d\lambda) \geq \tau \right\} \quad (3.1)$$

where the probability measure  $\mu$ , interval  $\Lambda = [\lambda_{\min}, \lambda_{\max}] \subseteq (0, \infty)$ , function  $f : [0, 1] \rightarrow \mathbb{R}$ , and threshold  $\tau$  are detailed in Section 3.2 below. Unlike the relatively coarse maximum criterion used by stability selection, the integral in Equation 3.1 incorporates information about the stability paths over a wide range of  $\lambda$  values. In Figure 2, for example, IPSS captures the fact that the stability paths of the true features rise at different rates, with some overtaking many of the false features more gradually than others, a point missed by MB, UM, and  $r$ -concave.

**3.2. Parameters.** The role of  $f$  in Equation 3.1 is to transform the selection probabilities  $\hat{\pi}_j$  to improve performance. Importantly, not all functions  $f$  can be used: To implement IPSS with a specific  $f$ , one must prove a corresponding bound on  $E(\text{FP})$ . Different functions yield different bounds, and tighter bounds often yield more true positives at the same target  $E(\text{FP})$ . Thus, functions with tighter bounds are generally more desirable. In Theorem 4.1, we establish upper bounds on  $E(\text{FP})$  for the class of functions

$$h_m(x) = (2x - 1)^m \mathbf{1}(x \geq 0.5), \quad (3.2)$$

where  $m \in \mathbb{N}$  (the  $h$  stands for ‘‘half’’, since  $h_m$  is nonzero on half the unit interval). We focus on this class—specifically IPSS with  $f = h_2$  and  $f = h_3$ , denoted IPSS(quad) and IPSS(cubic), respectively—because they yield the tightest bounds on  $E(\text{FP})$  among the many functions that we consider (Section S3). Simulation and real-data results in Section 5, Section 6, and the Supplement show that both methods routinely identify more true positives than all of the stability selection methods, consistent with the relative strengths of the theoretical bounds discussed in Section 4.3. Furthermore, IPSS(cubic) typically identifies at least as many true positives as IPSS(quad). The lone disadvantage of IPSS(cubic) relative to IPSS(quad) and stability selection is that its tighter  $E(\text{FP})$  bound makes it more sensitive to violations of Condition 1 (the only assumption besides iid samples that is required by Theorem 4.1), and thus more prone to overshooting the target  $E(\text{FP})$ . However, this primarily occurs in a subset of the logistic regression experiments (Figures S10 and S11), and even then the target  $E(\text{FP})$  is only exceeded by  $\leq 2$  false positives when  $p = 200$ , or  $\leq 4$  false positives when  $p = 1000$ . For comparison, cross-validation produces  $\geq 17$  false positives when  $p = 200$  and  $\geq 50$  false positives when  $p = 1000$  on the same data.

For IPSS, the interval  $\Lambda = [\lambda_{\min}, \lambda_{\max}]$  is defined as follows. The upper endpoint  $\lambda_{\max}$  is the same as in stability selection and equally inconsequential. The lower endpoint  $\lambda_{\min}$  is based on a bound of the form  $E(\text{FP}) \leq \mathcal{I}(\lambda, \lambda_{\max})/\tau$  that depends on  $f$ , where  $\mathcal{I}(\lambda, \lambda_{\max})$  is an integral over  $[\lambda, \lambda_{\max}]$  such as in Equations 4.4 and 4.5. Specifically, we define

$$\lambda_{\min} = \inf \left\{ \lambda \in (0, \lambda_{\max}) : \mathcal{I}(\lambda, \lambda_{\max}) \leq C \right\} \quad (3.3)$$

for a fixed cutoff,  $C$ . We always use  $C = 0.05$ , but extensive sensitivity analyses in Section S8.1 show that similar results are obtained for any choice of  $C$  over a wide range of settings, and that both IPSS methods outperform all versions of stability selection regardless of this choice. Further details about the construction of  $\Lambda$  and the evaluation of Equation 3.3 are in Section S1.1.

The probability measure  $\mu$  in Equation 3.1 weights different values of  $\lambda$ . While Theorems 4.1 and 4.2 hold for any choice  $\mu$ , we focus on the family of probability measures  $\mu_\alpha(d\lambda) \propto \lambda^{-\alpha} d\lambda$  parametrized by  $\alpha \in \mathbb{R}$ , as detailed in Section S1.2. The values  $\alpha = 0$  and  $\alpha = 1$  correspond to averaging over  $\Lambda$  on linear and log scales, respectively. Experiments in Section S8 show that larger values of  $\alpha$  generally yield more true positives, but are more likely to violate the  $E(FP)$  bound. This is because larger values of  $\alpha$  place greater weight on smaller regularization values, where Condition 1 is more likely to be violated; see Section S5. Nevertheless, both IPSS(quad) and IPSS(cubic) identify more true positives than all of the stability selection methods while still controlling  $E(FP)$  across a wide range of  $\alpha$  values (Section S8.2). As a general default,  $\alpha = 1$  works well. Other choices of  $\alpha$  based on known quantities—such as the base estimator or the number of features—can lead to even better performance; see Section S8.2.

The threshold  $\tau$  is determined by specifying a target  $E(FP)$ , denoted  $E(FP)_*$ , and replacing the inequality in Equation 4.2 with an equality, representing a worst-case scenario under the assumptions of Theorem 4.1. This gives  $\tau = \mathcal{I}(\Lambda)/E(FP)_*$  and Equation 3.1 becomes

$$\hat{S}_{\text{IPSS}} = \left\{ j : \int_{\Lambda} f(\hat{\pi}_j(\lambda)) \mu(d\lambda) \geq \frac{\mathcal{I}(\Lambda)}{E(FP)_*} \right\} = \left\{ j : E(FP)_* \geq \text{efp}(j) \right\} \quad (3.4)$$

where  $\mathcal{I}(\Lambda) = \mathcal{I}(\lambda_{\min}, \lambda_{\max})$  and, for each  $j \in \{1, \dots, p\}$ , the *efp score* of  $j$  is defined as

$$\text{efp}(j) = \min \left\{ \frac{\mathcal{I}(\Lambda)}{\int_{\Lambda} f(\hat{\pi}_j(\lambda)) \mu(d\lambda)}, p \right\}. \quad (3.5)$$

Under the assumptions of Theorem 4.1,  $\text{efp}(j)$  is the smallest bound on  $E(FP)$  if  $j$  is to be selected. The minimum in Equation 3.5 accounts for  $\int_{\Lambda} f(\hat{\pi}_j(\lambda)) \mu(d\lambda)$  being 0, in which case  $j$  is never selected since  $E(FP)$  is at most the number of features,  $p$ .

Equations 3.4 and 3.5 help to understand why IPSS does not depend strongly on  $\mu$  and  $C$  (which determines  $\Lambda$ ). The key quantity is  $\mathcal{I}(\Lambda)/\int_{\Lambda} f(\hat{\pi}_j(\lambda)) \mu(d\lambda)$ , in which the numerator and denominator are expectations with respect to  $\mu$  over  $\Lambda$ . IPSS depends primarily on the integrands of these functions, which are determined by the function  $f$ , rather than the probability measure  $\mu$  and its support  $\Lambda$ .

**3.3. Computation.** Algorithm 2 provides a step-by-step procedure for IPSS. Numerous works have noted that the number of subsampling iterations  $B$  is inconsequential provided it is sufficiently large (Shah and Samworth, 2013);  $B = 50$  is a common choice, and the one used throughout this work. The grid in Step 2 is used to accurately and efficiently approximate all integrals in the algorithm by simple Riemann sums (Proposition S1.1). We use  $r = 25$  grid points. Like many of the other parameters,  $r$  is inconsequential provided it is sufficiently large; in our experience, values greater than 15 suffice. This is because the functions  $h_m$ , the stability paths, the integrand in the upper bound  $\mathcal{I}(\Lambda)$ , and the measures  $\mu_\alpha$  are all very numerically stable. The bounds in Step 3 are in Theorem 4.2 for IPSS(quad) and IPSS(cubic). We find no discernible difference in computation time between IPSS and MB. This is because IPSS and MB both compute the  $\hat{\pi}_j$  using Algorithm 1, which is much more expensive than evaluation of either Equation 2.3 or Equation 3.1. For more on the computational requirements of Algorithm 1, see Meinshausen and Bühlmann (2010, Section 2.6).

---

**Algorithm 2** (Integrated path stability selection)

---

**Input:** Data  $\mathbf{z}_1, \dots, \mathbf{z}_n$ , selection algorithm  $\hat{S}$ , number of iterations  $B$ , function  $f$ , probability measure  $\mu$ , target  $E(FP)_*$ , integral cutoff value  $C$ , and number of grid points  $r$ .

- 1: Compute  $\lambda_{\min}$  and  $\lambda_{\max}$  as described above and in Section S1.1.
- 2: Partition  $\Lambda = [\lambda_{\min}, \lambda_{\max}]$  into  $r$  grid points, typically on a log scale.
- 3: Compute  $\mathcal{I}(\lambda_{\min}, \lambda_{\max})$  using the relevant upper bound on  $E(FP)$  and Proposition S1.1.
- 4: Estimate selection probabilities via Algorithm 1 with  $\mathbf{z}_1, \dots, \mathbf{z}_n$ ,  $\hat{S}$ ,  $\Lambda$ , and  $B$ .
- 5: Approximate  $\int_{\Lambda} f(\hat{\pi}_j(\lambda))\mu(d\lambda)$  using Proposition S1.1, then compute  $\text{efp}(j)$  using Equation 3.5.

**Output:** Selected features  $\hat{S}_{\text{IPSS},f} = \{j : \text{efp}(j) \leq E(FP)_*\}$ .

---

**3.4. False discovery rate.** IPSS and other forms of stability selection focus on  $E(FP)$  because it is interpretable and theoretically tractable. Another quantity of interest, the *false discovery rate* (FDR), is the expected ratio between the number of false positives and the total number of features selected,  $\text{FDR} = E(\text{FP}/(\text{TP} + \text{FP}))$ . When  $p$  is large, the FDR is well-approximated by  $E(\text{FP})/E(\text{TP} + \text{FP})$  (Storey and Tibshirani, 2003). Thus, making the additional approximation  $|\hat{S}_{\text{IPSS}}| \approx E(\text{TP} + \text{FP})$ , we have  $\text{FDR} \approx E(\text{FP})/|\hat{S}_{\text{IPSS}}|$ . Relabeling features by their efp scores so that  $\text{efp}(1) \leq \text{efp}(2) \leq \dots \leq \text{efp}(p)$ , the set of features  $\{1, \dots, j\}$  has an approximate FDR that is bounded above by  $\text{efp}(j)/j$  for each  $j \in \{1, \dots, p\}$ . Hence, instead of specifying  $E(FP)_*$ , one can either (i) specify a target FDR, say  $\text{FDR}_*$ , and choose the largest  $j$  such that  $\text{efp}(j)/j \leq \text{FDR}_*$ , or (ii) choose  $j$  to minimize  $\text{efp}(j)/j$ . The resulting set of selected features is then  $\{1, \dots, j\}$ , that is, the features with the  $j$  smallest efp scores.

---

 4. THEORY

---

In this section, we present our theoretical results (Section 4.2) and compare them to those of Meinshausen and Bühlmann (2010) and Shah and Samworth (2013) (Section 4.3). Our main result, Theorem 4.1, establishes a bound on  $E(FP)$  for IPSS with the functions  $h_m$  defined in Equation 3.2. Theorem 4.2 gives simplified formulas for this bound that we use in practice. All proofs are in Section S2. Additional results for other choices of  $f$  and their proofs are in Section S3.

**4.1. Preliminaries.** It is assumed that the random vectors  $\mathbf{Z}_1, \dots, \mathbf{Z}_n$ , the random subsets  $A_1, \dots, A_{2B}$ , and any randomness in the feature selection algorithm  $\hat{S}$  are defined on a common probability space  $(\Omega, \mathcal{F}, \mathbb{P})$ . Furthermore,  $E$  always denotes expectation with respect to  $\mathbb{P}$ . Let  $\Lambda$  be a Borel measurable subset of  $(0, \infty)$  equipped with the Borel sigma-algebra, let  $\mu$  be a probability measure on  $\Lambda$ , and assume  $\hat{S}_{\lambda}(\mathbf{Z}_A)$  is measurable as a function on  $\Lambda \times \Omega$  for all  $A \subseteq \{1, \dots, n\}$ .

**4.2. Main results.** The following condition is used in Theorem 4.1. Recall that  $S$  is the unknown subset of true features, and  $S^c = \{1, \dots, p\} \setminus S$  is its complement. Let  $q(\lambda) = E|\hat{S}_{\lambda}(\mathbf{Z}_{1:\lfloor n/2 \rfloor})|$  denote the expected number of features selected by  $\hat{S}_{\lambda}$  on half the data.

**Condition 1.** We say Condition 1 holds for  $m$  if for all  $\lambda \in \Lambda$ ,

$$\max_{j \in S^c} \mathbb{P} \left( j \in \bigcap_{b=1}^m (\hat{S}_{\lambda}(\mathbf{Z}_{A_{2b-1}}) \cap \hat{S}_{\lambda}(\mathbf{Z}_{A_{2b}})) \right) \leq (q(\lambda)/p)^{2m}. \quad (4.1)$$

Equation 4.1, discussed in greater detail below, says the probability that any non-true feature  $j$  is selected by both  $\hat{S}_\lambda(\mathbf{Z}_{A_{2b-1}})$  and  $\hat{S}_\lambda(\mathbf{Z}_{A_{2b}})$  in  $m$  resampling iterations is no greater than the  $2m$ -th power of the expected proportion of features selected by  $\hat{S}_\lambda$  using half the data.

**Theorem 4.1.** *Let  $\tau \in (0, 1]$  and  $m \in \mathbb{N}$ . Define  $\hat{S}_{\text{IPSS}, h_m}$  as in Equations 3.1 and 3.2. If Condition 1 holds for all  $m' \in \{1, \dots, m\}$ , then*

$$\mathbb{E}(\text{FP}) = \mathbb{E}|\hat{S}_{\text{IPSS}, h_m} \cap S^c| \leq \frac{p}{\tau B^m} \sum_{k_1 + \dots + k_B = m} \frac{m!}{k_1! k_2! \dots k_B!} \int_{\Lambda} (q(\lambda)/p)^{2 \sum_b \mathbb{1}(k_b \neq 0)} \mu(d\lambda) \quad (4.2)$$

where  $B$  is the number of subsampling steps in Algorithm 1 and the sum is over all nonnegative integers  $k_1, \dots, k_B$  such that  $k_1 + \dots + k_B = m$ .

Equation 4.2 bounds the expected number of false positives when using IPSS with  $h_m$ . The following theorem shows that the bound simplifies considerably for certain choices of  $m$ .

**Theorem 4.2.** *Let  $\tau \in (0, 1]$ . If Condition 1 holds for  $m = 1$ , then IPSS with  $h_1$  satisfies*

$$\mathbb{E}(\text{FP}) \leq \frac{1}{\tau} \int_{\Lambda} \frac{q(\lambda)^2}{p} \mu(d\lambda); \quad (4.3)$$

if Condition 1 holds for  $m \in \{1, 2\}$ , then IPSS with  $h_2$  satisfies

$$\mathbb{E}(\text{FP}) \leq \frac{1}{\tau} \int_{\Lambda} \left( \frac{q(\lambda)^2}{Bp} + \frac{(B-1)q(\lambda)^4}{Bp^3} \right) \mu(d\lambda); \quad (4.4)$$

and if Condition 1 holds for  $m \in \{1, 2, 3\}$ , then IPSS with  $h_3$  satisfies

$$\mathbb{E}(\text{FP}) \leq \frac{1}{\tau} \int_{\Lambda} \left( \frac{q(\lambda)^2}{B^2 p} + \frac{3(B-1)q(\lambda)^4}{B^2 p^3} + \frac{(B-1)(B-2)q(\lambda)^6}{B^2 p^5} \right) \mu(d\lambda). \quad (4.5)$$

Taking the limit as  $B \rightarrow \infty$ , Equations 4.4 and 4.5 become

$$\limsup_{B \rightarrow \infty} \mathbb{E}(\text{FP}) \leq \frac{1}{\tau p^3} \int_{\Lambda} q(\lambda)^4 \mu(d\lambda) \quad \text{and} \quad \limsup_{B \rightarrow \infty} \mathbb{E}(\text{FP}) \leq \frac{1}{\tau p^5} \int_{\Lambda} q(\lambda)^6 \mu(d\lambda). \quad (4.6)$$

Although we do not use these asymptotic bounds, the pattern from  $h_1$  (Equation 4.3) to  $h_2$  to  $h_3$  (Equation 4.6) provides insight into the relationships between  $\mathbb{E}(\text{FP})$ ,  $p$ , and  $h_m$ .

Condition 1 holds for  $m = 1$  whenever  $\max_{j \in S^c} \pi_j(\lambda) \leq q(\lambda)/p$  for all  $\lambda \in \Lambda$  since  $\mathbf{Z}_1, \dots, \mathbf{Z}_n$  are i.i.d. and independent of  $A_1, \dots, A_{2B}$ , and thus for any  $j \in S^c$ ,

$$\begin{aligned} \mathbb{P}(j \in \hat{S}_\lambda(\mathbf{Z}_{A_{2b-1}}) \cap \hat{S}_\lambda(\mathbf{Z}_{A_{2b}})) &= \mathbb{E}\left(\mathbb{E}\left(\mathbb{1}(j \in \hat{S}_\lambda(\mathbf{Z}_{A_{2b-1}})) \mathbb{1}(j \in \hat{S}_\lambda(\mathbf{Z}_{A_{2b}})) \mid A_{2b}, A_{2b-1}\right)\right) \\ &= \mathbb{E}(\pi_j(\lambda) \pi_j(\lambda)) = \pi_j(\lambda)^2 \leq (q(\lambda)/p)^2. \end{aligned} \quad (4.7)$$

In turn, the  $\max_{j \in S^c} \pi_j(\lambda) \leq q(\lambda)/p$  condition is implied by the exchangeability and not-worse-than-random-guessing conditions used by Meinshausen and Bühlmann (2010) and Shah and Samworth (2013) in the stability selection analogues of Theorem 4.1, detailed in Section 4.3. To be precise, Shah and Samworth (2013) do not require these conditions in their theory, but they are always assumed when implementing their versions of stability selection in practice. An empirical study and further details about Condition 1 for the practically relevant cases of  $m \in \{1, 2, 3\}$  are in Section S5.

**4.3. Comparison to stability selection.** The analogue of Equation 4.2 for stability selection (Equation 2.3) under the exchangeability and not-worse-than-random-guessing conditions of Meinshausen and Bühlmann (2010) is

$$E(FP) \leq \frac{q_\Lambda^2}{(2\tau - 1)p}, \quad (4.8)$$

where  $q_\Lambda = E|\bigcup_{\lambda \in \Lambda} \hat{S}_\lambda(\mathbf{Z}_{1:\lfloor n/2 \rfloor})|$ . Under the additional assumptions that (a)  $q(\lambda)^2/p \leq 1/\sqrt{3}$  for all  $\lambda \in \Lambda$  and (b) the distributions of the simultaneous selection probabilities (defined in Section S2) are unimodal, Shah and Samworth (2013) establish the stronger bound

$$E(FP) \leq \frac{C(\tau, B) q_\Lambda^2}{p} \quad (4.9)$$

for stability selection where, for  $\tau \in \{\frac{1}{2} + 1/B, \frac{1}{2} + 3/(2B), \frac{1}{2} + 2/B, \dots, 1\}$ ,

$$C(\tau, B) = \begin{cases} \frac{1}{2(2\tau - 1 - \frac{1}{2B})} & \text{if } \tau \in \left( \min \left\{ \frac{1}{2} + \frac{q_\Lambda^2}{p^2}, \frac{1}{2} + \frac{1}{2B} + \frac{3q_\Lambda^2}{4p^2} \right\}, 3/4 \right], \\ \frac{4(1 - \tau + \frac{1}{2B})}{1 + \frac{1}{B}} & \text{if } \tau \in (3/4, 1]. \end{cases}$$

There are several reasons the IPSS bounds in Theorem 4.2 are significantly tighter than the Meinshausen and Bühlmann (MB) and unimodal (UM) bounds in Equations 4.8 and 4.9. First, the IPSS bounds hold for all  $\tau \in (0, 1]$ , whereas the MB and UM bounds are restricted to  $\tau \in (0.5, 1]$  since they go to  $\infty$  as  $\tau \rightarrow 0.5$ . Second, all of the terms in the integrands of Equations 4.4 and 4.5 are typically orders of magnitude smaller than  $q^2/p$  in both Equations 4.8 and 4.9. Indeed, since  $\max\{q(\lambda) : \lambda \in \Lambda\} \leq q_\Lambda$  and  $q(\lambda)$  is much smaller than  $p$  over a wide range of  $\lambda$  values in sparse or even moderately sparse settings,  $q(\lambda)^4/p^3$  and  $q(\lambda)^6/p^5$  are typically much smaller than  $q_\Lambda^2/p$ , and this difference becomes more pronounced as  $p$  grows. Additionally, the lower order terms in Equations 4.4 and 4.5 are  $O(1/B)$  or  $O(1/B^2)$ , so with our typical choice of  $B = 50$ , the contribution of these terms is reduced even further, tending to 0 as  $B \rightarrow \infty$  (Equation 4.6). By contrast, the MB bound has no  $B$  dependence, and the UM bound depends only weakly on  $B$ .

Shah and Samworth (2013) also derive an upper bound based on assumptions of  $r$ -concavity. They argue that if the estimated selection probabilities are  $-1/4$ -concave and the simultaneous selection probabilities (Section S2) are  $-1/2$ -concave for every feature in  $S^c$ , then

$$E(FP) \leq \min \left\{ D(q_\Lambda^2/p^2, 2\tau - 1, B, -1/2), D(q_\Lambda/p, \tau, 100, -1/4) \right\} p \quad (4.10)$$

where  $D(\eta, \tau, B, r)$  is the maximum of  $\mathbb{P}(X \geq \tau)$  over all  $r$ -concave random variables  $X$  that are supported on  $\{0, 1/B, 2/B, \dots, 1\}$  and satisfy  $\mathbb{E}(X) \leq \eta$  (Shah and Samworth, 2013). While tighter than the MB and UM bounds, the function  $D$ —and hence, the upper bound in Equation 4.10—does not have a closed form and must be approximated with an additional algorithm. This lack of a closed-form expression and the constrained maximization over all  $r$ -concave random variables makes it difficult to compare the  $r$ -concave bound with Equations 4.2, 4.8, and 4.9 analytically. However, the results in Figure 3 indicate that our bounds for IPSS(quad) and IPSS(cubic) are tighter than all of the stability selection bounds—including  $r$ -concave—especially for target  $E(FP)$  values less than 5, which is the most practically relevant range. Furthermore, our empirical results show that IPSS(quad) and IPSS(cubic) consistently identify more true positives than  $r$ -concave while maintaining  $E(FP)$  control across many diverse settings. Thus, while  $r$ -concave is less conservative than other traditional approaches, it requires stronger assumptions, relies on an additional algorithm due to lack of a closed form, and routinely underperforms IPSS.

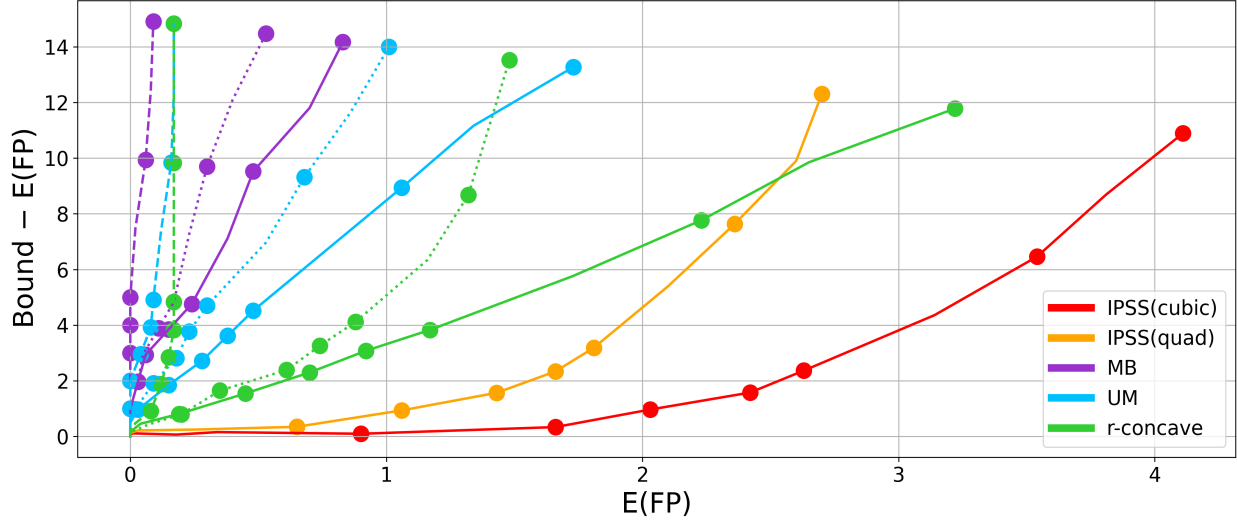


FIGURE 3. *Tightness of the  $E(FP)$  bounds.* The difference between the theoretical  $E(FP)$  bound for each method and its actual  $E(FP)$ , averaged over 100 data sets simulated from an independent linear regression model with normal residuals and  $p = 200$  features, as described in Section 5, versus actual  $E(FP)$ . Since all methods replace the inequalities in their  $E(FP)$  bounds with equalities, a perfectly calibrated method would generate a horizontal line at 0, that is,  $E(FP) = \text{Bound}$ . Dots show the results for each method when  $E(FP)_*$  equals, from left to right, 1, 2, 3, 4, 5, 10, and 15. IPSS(quad) and especially IPSS(cubic) are much closer to their theoretical bounds, particularly when  $E(FP)_* \leq 5$ . Solid, dotted, and dashed lines for the stability selection methods correspond to  $\tau = 0.6, 0.75$ , and  $0.9$ , respectively.

---

## 5. SIMULATIONS

---

We present results from linear and logistic regression simulations for a variety of feature distributions and base estimators. The performance of IPSS is compared to the stability selection methods of Meinshausen and Bühlmann (2010) and Shah and Samworth (2013), as well as cross-validation.

*Setup.* Data are simulated from a linear regression model with normal residuals:

$$Y_i = \mathbf{X}_i^T \boldsymbol{\beta}^* + \epsilon_i, \quad \epsilon_i \sim \mathcal{N}(0, \sigma^2),$$

from a linear model with residuals from a Student's  $t$  distribution with 2 degrees of freedom:

$$Y_i = \mathbf{X}_i^T \boldsymbol{\beta}^* + \epsilon_i, \quad \epsilon_i \sim t(2),$$

and from a binary logistic regression model:

$$Y_i \sim \text{Bernoulli}(p_i), \quad p_i = \frac{\exp(\gamma \mathbf{X}_i^T \boldsymbol{\beta}^*)}{1 + \exp(\gamma \mathbf{X}_i^T \boldsymbol{\beta}^*)},$$

for  $i \in \{1, \dots, n\}$ . For each simulated data set, the coefficient vector  $\boldsymbol{\beta}^*$  has  $s$  nonzero entries  $\beta_j^* \sim \text{Uniform}([-1, -0.5] \cup [0.5, 1])$  located at randomly chosen coordinates  $j \in \{1, \dots, p\}$ , and the remaining  $p - s$  entries are set to 0. We simulate features from the following designs:

- *Independent:*  $\mathbf{X}_i \sim \mathcal{N}(0, I_p)$  for all  $i$ , where  $I_p$  is the  $p \times p$  identity matrix.

- *Toeplitz*:  $\mathbf{X}_i \sim \mathcal{N}(0, \Sigma)$  where  $\Sigma_{jk} = \rho^{|j-k|}$ . We consider two cases:  $\rho = 0.5$  and  $\rho = 0.9$ .
- *RNA-seq*:  $n$  samples and  $p$  features are drawn uniformly at random from RNA-sequencing measurements of 6426 genes from 569 ovarian cancer patients (Vasaikar et al., 2018).

For each  $j \in \{1, \dots, p\}$ , we standardize the observed features  $(x_{1j}, \dots, x_{nj})$  to have sample mean 0 and sample variance 1 before applying  $\hat{S}_\lambda$ . For linear regression, the observed response  $y = (y_1, \dots, y_n)$  is centered to have sample mean 0. For linear regression with normal residuals,  $\sigma^2$  is chosen to satisfy a specified empirical signal-to-noise ratio (SNR), defined by  $\text{SNR} = \sum_{i=1}^n (\mathbf{x}_i^\top \boldsymbol{\beta}^*)^2 / (n\sigma^2)$ . For logistic regression,  $\gamma > 0$  determines the strength of the signal.

The three models (linear regression with normal and Student's  $t$  residuals, and logistic regression), four feature designs (independent, Toeplitz with  $\rho = 0.5$  and 0.9, and RNA-seq), and two feature dimensions ( $p = 200$  and 1000) yield a total of 24 simulation settings. For linear regression, we perform experiments with lasso, MCP, SCAD, and the adaptive lasso as the base estimators, and for logistic regression the base estimator is  $\ell_1$ -regularized logistic regression. For IPSS, the parameter  $C$  is always set to 0.05 and  $\alpha$  is set to the default values described in Section S8.2. Each experiment consists of 100 trials, where one trial consists of generating data as above with  $n$ ,  $s$ , and signal strength chosen according to Table 1, estimating the selection probabilities via Algorithm 1 with  $B = 50$  subsamples, and choosing features according to each criterion.

$p$	$n$	$s$	SNR (regression)	$\gamma$ (classification)
200	Uniform{50, ..., 200}	Uniform{5, ..., 20}	Uniform(1/3, 3)	Uniform(1/2, 2)
1000	Uniform{100, ..., 500}	Uniform{10, ..., 40}	Uniform(1/3, 3)	Uniform(1/2, 2)

TABLE 1. *Simulation parameters*. The number of samples  $n$ , number of true features  $s$ , and the signal strength parameters, SNR and  $\gamma$ , are randomly selected prior to each trial as above, ensuring that our experiments cover a wide range of settings.

*Results.* We quantify performance in terms of true positives (TP) and false positives (FP), where a selected feature is a *true positive* if its corresponding  $\boldsymbol{\beta}^*$  entry is nonzero, and is a *false positive* otherwise. The dashed black line in each FP plot shows the target value of  $E(\text{FP})$ . A tight bound on  $E(\text{FP})$  should lead to curves lying close to this line, since all methods replace the inequalities in their respective  $E(\text{FP})$  bounds with equalities to calibrate the parameters. For example, if the target  $E(\text{FP})$  is 2, a perfectly calibrated algorithm would produce an average FP of 2.

Figures 4 and 5 show results for linear regression with normal residuals and lasso as the base estimator when  $p = 200$  and 1000. Results are shown for IPSS and the stability selection methods as well as lasso, MCP, and SCAD with their regularization parameters by cross-validation (lassoCV, MCPCV, and SCADCV). The remaining results are in Section S7. Figures S2 and S3 show results for linear regression with Student's  $t$  residuals and lasso as the base estimator, Figures S4 and S5 show results for linear regression with normal residuals and MCP as the base estimator, Figures S6 and S7 show results for linear regression with normal residuals and SCAD as the base estimator, Figures S8 and S9 show results for linear regression with normal residuals and the adaptive lasso as the base estimator, and Figures S10 and S11 show results for logistic regression with  $\ell_1$ -regularized logistic regression as the base estimator.

In all 48 experiments, IPSS(quad) achieves more accurate  $E(\text{FP})$  control and identifies more true positives than all of the stability selection methods, often substantially so. IPSS(cubic) also achieves more accurate  $E(\text{FP})$  control and identifies more true positives than the stability selection methods

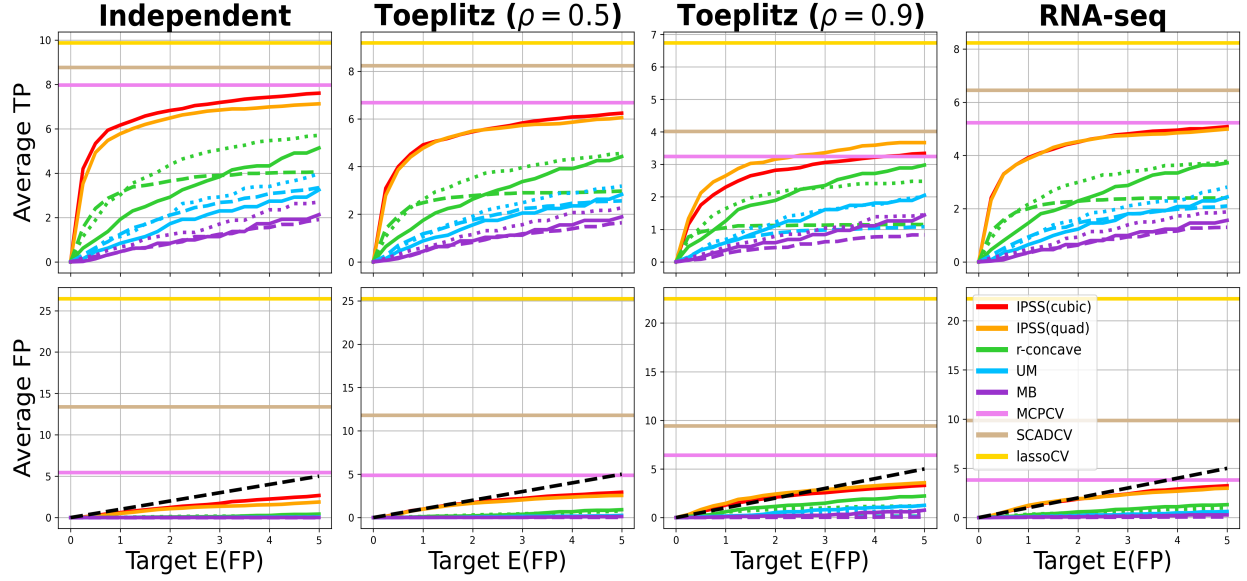


FIGURE 4. *Linear regression, normal residuals ( $p = 200$ )*. The solid, dotted, and dashed lines for the stability selection methods represent  $\tau = 0.6, 0.75$ , and  $0.9$ , respectively. Cross-validation results (horizontal lines) are independent of Target E(FP). The dashed black line represents perfect E(FP) control.

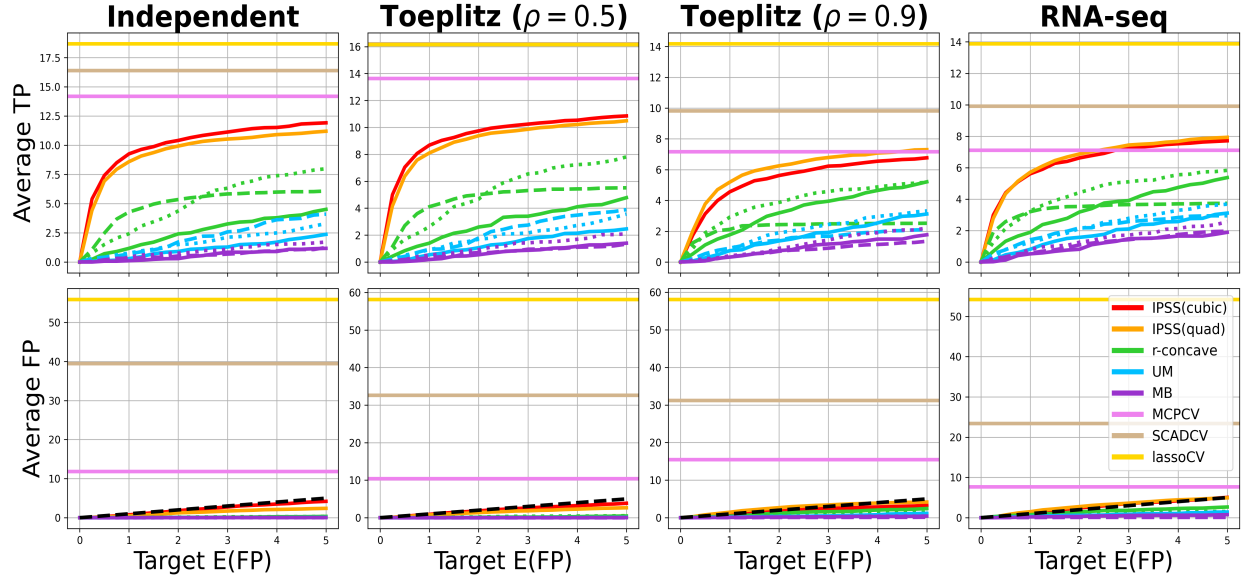


FIGURE 5. *Linear regression, normal residuals ( $p = 1000$ )*. See Figure 4 for details.

in almost every experiment, though—as discussed in Section 3.2—its empirical E(FP) slightly exceeds the target E(FP) in a few cases, notably logistic regression with Toeplitz ( $\rho = 0.9$ ) and RNA-seq designs. This is because violations of Condition 1 are more likely for  $\ell_1$ -regularized logistic regression than for lasso, MCP, SCAD, or the adaptive lasso. One possible explanation for this—which agrees with our empirical observations—is that  $\ell_1$ -regularized logistic regression can encounter computational difficulties at small regularization values when  $p \gg n$ , leading to

suboptimal solutions and hence poorly estimated selection probabilities (Friedman et al., 2010). Among the cross-validation methods, lassoCV and SCADCV have a high TP, but also exceedingly high FP. MCPCV does better in terms of limiting the number of false positives, but not as well as IPSS and stability selection. In some experiments, IPSS even identifies more true positives than MCPCV while selecting fewer false positives.

Figures 4 and 5 and the results in Section S7 indicate that IPSS provides a better balance between true and false positives across a wide range of settings and base estimators than stability selection and cross-validation. That is, while stability selection has low FP at the expense of low TP, and cross-validation has high TP at the expense of high FP, IPSS stays at or below the target  $E(FP)$  while achieving a TP that can approach or even surpass the TP of cross-validation.

---

## 6. APPLICATIONS

---

**6.1. Prostate cancer.** We applied IPSS and the stability selection methods to reverse-phase protein array (RPPA) measurements of  $p = 125$  proteins in  $n = 351$  prostate cancer patients (Vasaikar et al., 2018). The response is *tumor purity*—the proportion of cancerous cells in a tissue sample—and the goal is to identify the genes that are most related to it. Since tumor purity takes values in  $[0, 1]$ , we use lasso as our base selection algorithm. The target  $E(FP)$  is 1 for all methods, and for MB, UM, and  $r$ -concave we set  $\tau = 0.75$ . Figure 6 shows the results. MB, UM,  $r$ -concave, IPSS(quad), and IPSS(cubic) select 4, 4, 5, 8, and 10 proteins, respectively. Although it is difficult to know which features should be selected on real data such as this, a literature search presented in Section S6 indicates that all 10 proteins identified by IPSS play a nontrivial role in prostate cancer. As in Figure 2, the stability selection methods miss important information about the stability paths that IPSS successfully captures. For example, the selection probabilities for PKC, BAK1, and PTEN are essentially 0 for many  $\lambda$  values before abruptly rising above many of the other paths.

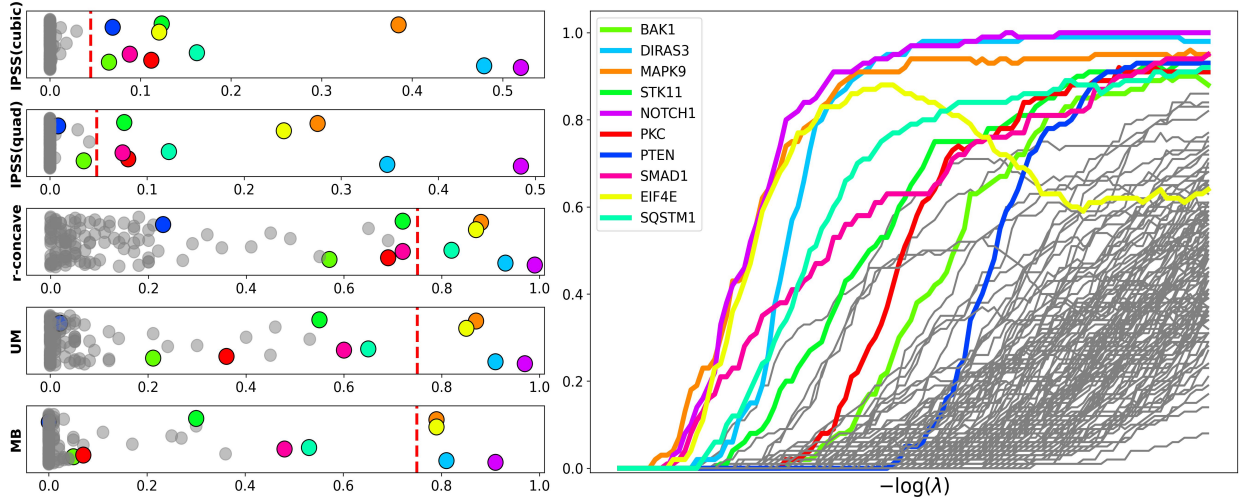


FIGURE 6. *Prostate cancer results.* (Left) Feature scores and thresholds (vertical red lines) separating selected and unselected genes for each method. Scores are one-dimensional and correspond to the horizontal axes. Every method’s set of selected proteins is a subset of the proteins selected by IPSS(cubic), shown in color in all plots; the remaining proteins are in gray. (Right) Estimated stability paths for each protein. The horizontal axis is on a log scale.

**6.2. Colon cancer.** We applied IPSS and stability selection to the expression levels of  $p = 1908$  genes in  $n = 62$  tissue samples, 40 cancerous and 22 normal (Alon et al., 1999). The goal is to identify genes whose expression levels differ between the cancerous and normal samples. Since the response is binary, we use  $\ell_1$ -regularized logistic regression as the base estimator. The target  $E(FP)$  is  $1/2$  for all methods, and the threshold for MB, UM, and  $r$ -concave is  $\tau = 0.75$ . Expression levels are log-transformed and standardized as in Shah and Samworth (2013), who also study these data. Figures 7 and 8 show the results. MB, UM,  $r$ -concave, IPSS(quad), and IPSS(cubic) select 1, 2, 7, 11, and 16 genes, respectively. In addition to Figure 8, a literature search reported in Section S6 supports the claim that the genes identified by IPSS are related to colon cancer.

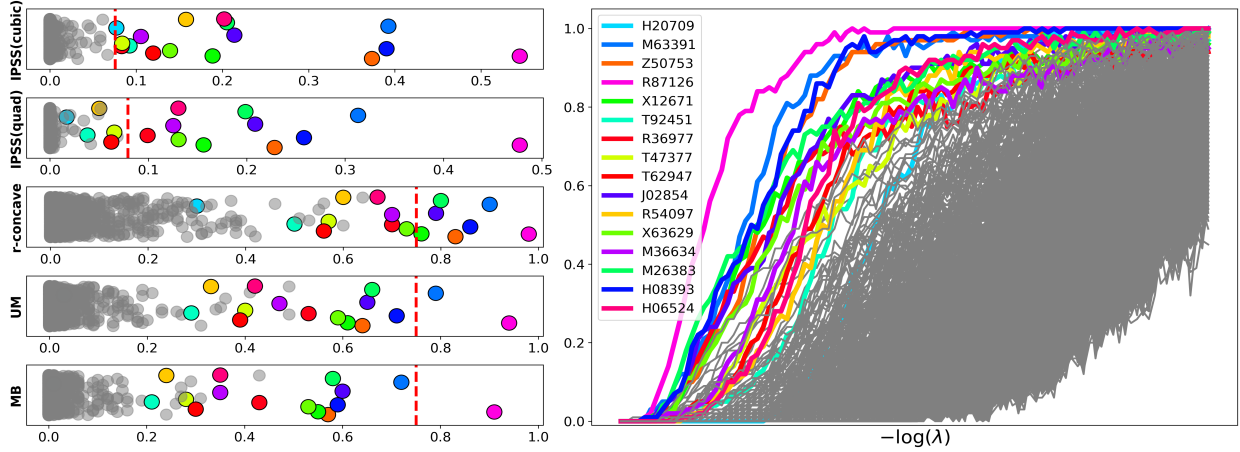


FIGURE 7. *Colon cancer results.* (Left) Feature scores and thresholds (vertical red lines) separating selected and unselected genes. Every method’s set of selected genes is a subset of those selected by IPSS(cubic), shown in color in all plots; the remaining genes are in gray. (Right) Estimated stability paths for each gene.

---

## 7. DISCUSSION

---

IPSS has several attractive properties. It has stronger theoretical guarantees than stability selection and significantly better performance on a wide range of simulated and real data. It also uses the same selection probabilities as stability selection and therefore has the same computational cost. In this work, we focused on the functions  $f = h_2$  and  $f = h_3$  due to their favorable theoretical properties and empirical performance. However, it is possible that other functions will lead to better results; investigating this point is an interesting line of future work. We also focused on the family of probability measures  $\mu_\alpha \propto \lambda^{-\alpha} d\lambda$  and provided guidance on choosing  $\alpha$ . Like  $f$ , it is possible that other means of selecting  $\alpha$  or other choices of  $\mu$  might lead to further improvements in performance. Notably, Theorems 4.1 and 4.2 and the theorems in Section S3 hold for arbitrary probability measures  $\mu$ , providing considerable flexibility in this choice.

Another interesting direction is to apply IPSS with other base estimators, such as graphical lasso and elastic net (Friedman et al., 2008; Zou and Hastie, 2005). In the case of elastic net, there are two regularization parameters, and while our methodology appears to carry over to this setting (now with  $\Lambda \subseteq (0, \infty)^2$  and  $(\lambda_1, \lambda_2) \mapsto \hat{S}_{\lambda_1, \lambda_2}$ ), it remains to work out the details and investigate the performance of IPSS in the context of multiple regularization parameters. Finally, we noted in Section 2.3 that stability selection is often used in conjunction with other statistical methods.

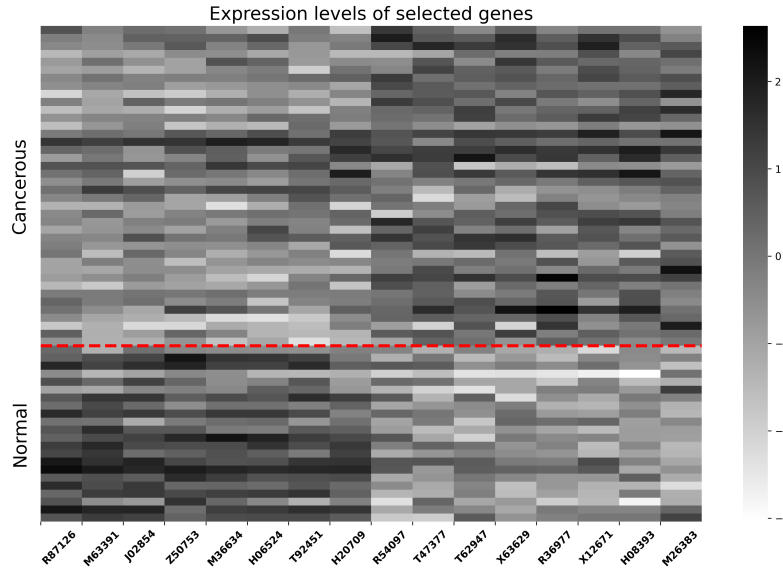


FIGURE 8. *Expression level heatmap for the 16 genes selected by IPSS(cubic)*. Each of the 62 rows corresponds to one tissue sample. The first 40 rows are cancerous, and the latter 22 are normal; the dashed red line separates the two classes. Each column corresponds to a gene selected by IPSS(cubic), or equivalently, the union of genes selected by each method since each gene selected by the other methods was also selected by IPSS(cubic). For each gene, there is a clear distinction between expression levels for cancerous versus normal samples.

Given that IPSS yields better results than stability selection at no additional cost and with less tuning, it would be interesting to study these joint methods with IPSS in place of stability selection.

---

#### DATA AND CODE AVAILABILITY

---

All datasets and code from this work are available at [https://github.com/omelikechi/ipss\\_jasa](https://github.com/omelikechi/ipss_jasa). Original datasets can be accessed at the following links: ovarian cancer ([https://www.linkedomics.org/data\\_download/TCGA-OV/](https://www.linkedomics.org/data_download/TCGA-OV/)); prostate cancer ([https://www.linkedomics.org/data\\_download/TCGA-PRAD](https://www.linkedomics.org/data_download/TCGA-PRAD)); and colon cancer (<http://genomics-pubs.princeton.edu/oncology/affydata/index.html>).

---

#### ACKNOWLEDGMENTS

---

O.M. thanks David Dunson and Steven Winter for initial discussions that took place under funding from Merck & Co. and the National Institutes of Health (NIH) grant R01ES035625. J.W.M. was supported in part by the National Institutes of Health (NIH) grant R01CA240299.

---

#### DISCLOSURE STATEMENT

---

The authors report there are no competing interests to declare.

---

## REFERENCES

---

David H Alexander and Kenneth Lange. Stability selection for genome-wide association. *Genetic Epidemiology*, 35(7):722–728, 2011.

Uri Alon, Naama Barkai, Daniel A Notterman, Kurt Gish, Suzanne Ybarra, Daniel Mack, and Arnold J Levine. Broad patterns of gene expression revealed by clustering analysis of tumor and normal colon tissues probed by oligonucleotide arrays. *Proceedings of the National Academy of Sciences*, 96(12):6745–6750, 1999.

Gangga Anuraga, Wan-Chun Tang, Nam Nhut Phan, Hoang Dang Khoa Ta, Yen-Hsi Liu, Yung-Fu Wu, Kuen-Haur Lee, and Chih-Yang Wang. Comprehensive analysis of prognostic and genetic signatures for general transcription factor III (GTF3) in clinical colorectal cancer patients using bioinformatics approaches. *Current Issues in Molecular Biology*, 43(1):2–20, 2021.

Georgia Arentz, Tim Chataway, Timothy J Price, Zaipul Izwan, Gemma Hardi, Adrian G Cummins, and Jennifer E Hardingham. Desmin expression in colorectal cancer stroma correlates with advanced stage disease and marks angiogenic microvessels. *Clinical Proteomics*, 8(1):1–13, 2011.

Francis R Bach. Bolasso: model consistent lasso estimation through the bootstrap. In *Proceedings of the 25th international conference on Machine learning*, pages 33–40, 2008.

Q. Bertrand, Q. Klopfenstein, P.-A. Bannier, G. Gidel, and M. Massias. Beyond L1: Faster and better sparse models with skglm. In *NeurIPS*, 2022.

Yumin Chen, Zunjun Zhang, Jianzhong Zheng, Ying Ma, and Yu Xue. Gene selection for tumor classification using neighborhood rough sets and entropy measures. *Journal of Biomedical Informatics*, 67:59–68, 2017.

Leandro S D'Abrono and Paramita M Ghosh. eIF4E phosphorylation in prostate cancer. *Neoplasia*, 20(6):563–573, 2018.

Jianqing Fan and Runze Li. Variable selection via nonconcave penalized likelihood and its oracle properties. *Journal of the American Statistical Association*, 96(456):1348–1360, 2001.

Jerome Friedman, Trevor Hastie, and Robert Tibshirani. Sparse inverse covariance estimation with the graphical lasso. *Biostatistics*, 9(3):432–441, 2008.

Jerome H Friedman, Trevor Hastie, and Rob Tibshirani. Regularization paths for generalized linear models via coordinate descent. *Journal of Statistical Software*, 33:1–22, 2010.

Valentina Grossi, Giuseppe Lucarelli, Giovanna Forte, Alessia Peserico, Antonio Matrone, Aldo Germani, Monica Rutigliano, Alessandro Stella, Rosanna Bagnulo, Daria Loconte, et al. Loss of STK11 expression is an early event in prostate carcinogenesis and predicts therapeutic response to targeted therapy against MAPK/p38. *Autophagy*, 11(11):2102–2113, 2015.

Anne-Claire Haury, Fantine Mordelet, Paola Vera-Licona, and Jean-Philippe Vert. TIGRESS: trustful inference of gene regulation using stability selection. *BMC Systems Biology*, 6(1):1–17, 2012.

Arthur E Hoerl and Robert W Kennard. Ridge regression: Biased estimation for nonorthogonal problems. *Technometrics*, 12(1):55–67, 1970.

Benjamin Hofner, Luigi Boccuto, and Markus Göker. Controlling false discoveries in high-dimensional situations: boosting with stability selection. *BMC Bioinformatics*, 16:1–17, 2015.

Jianfeng Huang, Angeles Duran, Miguel Reina-Campos, Tania Valencia, Elias A Castilla, Timo D Müller, Matthias H Tschöp, Jorge Moscat, and Maria T Diaz-Meco. Adipocyte p62/SQSTM1 suppresses tumorigenesis through opposite regulations of metabolism in adipose tissue and tumor. *Cancer Cell*, 33(4):770–784, 2018.

Tamara Jamaspishvili, David M Berman, Ashley E Ross, Howard I Scher, Angelo M De Marzo, Jeremy A Squire, and Tamara L Lotan. Clinical implications of PTEN loss in prostate cancer. *Nature Reviews Urology*, 15(4):222–234, 2018.

Adel Javanmard and Andrea Montanari. Confidence intervals and hypothesis testing for high-dimensional regression. *The Journal of Machine Learning Research*, 15(1):2869–2909, 2014.

Chenlei Leng, Yi Lin, and Grace Wahba. A note on the lasso and related procedures in model selection. *Statistica Sinica*, pages 1273–1284, 2006.

Albert Levy, Rivka Gal, Ruth Granoth, Zeev Dreznik, Mati Fridkin, and Illana Gozes. In vitro and in vivo treatment of colon cancer by VIP antagonists. *Regulatory Peptides*, 109(1-3):127–133, 2002.

Jun-Li Li and Chun-Xia Zhang. Ensembling variable selectors by stability selection for the Cox model. In *2017 International Conference on Machine Learning and Cybernetics (ICMLC)*, volume 1, pages 35–41. IEEE, 2017.

Shuang Li, Li Hsu, Jie Peng, and Pei Wang. Bootstrap inference for network construction with an application to a breast cancer microarray study. *The Annals of Applied Statistics*, 7(1):391, 2013.

Zhenqiu Liu, Ming Tan, and Feng Jiang. Regularized F-measure maximization for feature selection and classification. *BioMed Research International*, 2009(1):617946, 2009.

Suryanarayana Maddu, Bevan L Cheeseman, Ivo F Sbalzarini, and Christian L Müller. Stability selection enables robust learning of differential equations from limited noisy data. *Proceedings of the Royal Society A*, 478(2262):20210916, 2022.

Julien Mairal and Bin Yu. Complexity analysis of the lasso regularization path. *arXiv preprint arXiv:1205.0079*, 2012.

Nicolai Meinshausen and Peter Bühlmann. Stability selection. *Journal of the Royal Statistical Society Series B: Statistical Methodology*, 72(4):417–473, 2010.

Samira Nomiri, Reyhane Hoshyar, Elham Chamani, Zohreh Rezaei, Fatemeh Salmani, Pegah Larki, Tahmine Tavakoli, Neda Jalili Tabrizi, Afshin Derakhshani, Mariacarmela Santarpia, et al. Prediction and validation of GUCA2B as the hub-gene in colorectal cancer based on co-expression network analysis: In-silico and in-vivo study. *Biomedicine & Pharmacotherapy*, 147:112691, 2022.

Fabian Pedregosa, Gaël Varoquaux, Alexandre Gramfort, Vincent Michel, Bertrand Thirion, Olivier Grisel, Mathieu Blondel, Peter Prettenhofer, Ron Weiss, Vincent Dubourg, et al. Scikit-learn: Machine learning in Python. *Journal of Machine Learning Research*, 12:2825–2830, 2011.

Tao Qiu, William E Grizzle, Denise K Oelschlager, Xing Shen, and Xu Cao. Control of prostate cell growth: BMP antagonizes androgen mitogenic activity with incorporation of MAPK signals in Smad1. *The EMBO Journal*, 26(2):346–357, 2007.

Meghan A Rice, En-Chi Hsu, Merve Aslan, Ali Ghoochani, Austin Su, and Tanya Stoyanova. Loss of Notch1 activity inhibits prostate cancer growth and metastasis and sensitizes prostate cancer cells to antiandrogen therapies. *Molecular Cancer Therapeutics*, 18(7):1230–1242, 2019.

Gonzalo Rodríguez-Berriguete, Benito Fraile, Pilar Martínez-Onsurbe, Gabriel Olmedilla, Ricardo Paniagua, and Mar Royuela. MAP kinases and prostate cancer. *Journal of Signal Transduction*, 2012, 2012.

Rajen D Shah and Richard J Samworth. Variable selection with error control: another look at stability selection. *Journal of the Royal Statistical Society Series B: Statistical Methodology*, 75(1):55–80, 2013.

Xu-Bao Shi, Lingru Xue, Joy Yang, Ai-Hong Ma, Jianjun Zhao, Ma Xu, Clifford G Tepper, Christopher P Evans, Hsing-Jien Kung, and Ralph W deVere White. An androgen-regulated mirna suppresses Bak1 expression and induces androgen-independent growth of prostate cancer cells. *Proceedings of the National Academy of Sciences*, 104(50):19983–19988, 2007.

John D Storey and Robert Tibshirani. Statistical significance for genomewide studies. *Proceedings of the National Academy of Sciences*, 100(16):9440–9445, 2003.

Lichao Sun, Hai Hu, Liang Peng, Zhuan Zhou, Xuan Zhao, Jian Pan, Lixin Sun, Zhihua Yang, and Yuliang Ran. P-cadherin promotes liver metastasis and is associated with poor prognosis in colon cancer. *The American Journal of Pathology*, 179(1):380–390, 2011.

Margie N Sutton, Zhen Lu, Yao-Cheng Li, Yong Zhou, Tao Huang, Albert S Reger, Amy M Hurwitz, Timothy Palzkill, Craig Logsdon, Xiaowen Liang, et al. DIRAS3 (ARHI) blocks RAS/MAPK signaling by binding directly to RAS and disrupting RAS clusters. *Cell Reports*, 29(11):3448–3459, 2019.

Yuichi Tanaka, M Veronica Gavrielides, Yasuhiro Mitsuuchi, Teruhiko Fujii, and Marcelo G Kazanietz. Protein kinase C promotes apoptosis in LNCaP prostate cancer cells through activation of p38 MAPK and inhibition of the Akt survival pathway. *Journal of Biological Chemistry*, 278(36): 33753–33762, 2003.

Robert Tibshirani. Regression shrinkage and selection via the lasso. *Journal of the Royal Statistical Society Series B: Statistical Methodology*, 58(1):267–288, 1996.

Mitsunori Ushigome, Tsuneyuki Ubagai, Hirokazu Fukuda, Naoto Tsuchiya, Takashi Sugimura, Jun Takatsuka, and Hitoshi Nakagama. Up-regulation of hnRNP A1 gene in sporadic human colorectal cancers. *International Journal of Oncology*, 26(3):635–640, 2005.

Suhas V Vasaikar, Peter Straub, Jing Wang, and Bing Zhang. LinkedOmics: analyzing multi-omics data within and across 32 cancer types. *Nucleic Acids Research*, 46(D1):D956–D963, 2018.

Fan Wang, Sach Mukherjee, Sylvia Richardson, and Steven M Hill. High-dimensional regression in practice: an empirical study of finite-sample prediction, variable selection and ranking. *Statistics and Computing*, 30:697–719, 2020.

Shu-Lin Wang, Xueling Li, Shanwen Zhang, Jie Gui, and De-Shuang Huang. Tumor classification by combining PNN classifier ensemble with neighborhood rough set based gene reduction. *Computers in Biology and Medicine*, 40(2):179–189, 2010.

Shulin Wang, Huowang Chen, Renfa Li, and Dingxing Zhang. Gene selection with rough sets for the molecular diagnosing of tumor based on support vector machines. 2006.

Cun-Hui Zhang. Nearly unbiased variable selection under minimax concave penalty. *The Annals of Statistics*, 38(2):894–942, 2010.

Jiwei Zhang, Shengli Li, Ling Zhang, Juan Xu, Mingxu Song, Tingting Shao, Zhaohui Huang, and Yongsheng Li. RBP EIF2S2 promotes tumorigenesis and progression by regulating MYC-mediated inhibition via FHIT-related enhancers. *Molecular Therapy*, 28(4):1105–1118, 2020.

Jiayu Zhou, Jimeng Sun, Yashu Liu, Jianying Hu, and Jieping Ye. Patient risk prediction model via top-k stability selection. In *Proceedings of the 2013 SIAM International Conference on Data Mining*, pages 55–63. SIAM, 2013.

Hui Zou. The adaptive lasso and its oracle properties. *Journal of the American Statistical Association*, 101(476):1418–1429, 2006.

Hui Zou and Trevor Hastie. Regularization and variable selection via the elastic net. *Journal of the Royal Statistical Society Series B: Statistical Methodology*, 67(2):301–320, 2005.

## SUPPLEMENTARY MATERIAL

We provide further details on the implementation of IPSS (Section S1), prove Theorems 4.1 and 4.2 (Section S2), state and prove results for IPSS with functions that are not considered in the main text (Section S3), describe using IPSS with other base estimators (Section S4), and provide an empirical study of Condition 1 (Section S5), additional results from the prostate and colon cancer applications (Section S6) and simulation experiments (Section S7), and a sensitivity analysis of the IPSS parameters,  $C$  and  $\alpha$  (Section S8).

---

### S1. ALGORITHMIC DETAILS

---

We elaborate on the construction of the interval  $\Lambda$  for IPSS (Section S1.1) and describe a simple way to approximate the integrals in the IPSS criterion (Equation 3.1) for a wide range of functions  $f$  and measures  $\mu$  (Section S1.2).

**S1.1. Constructing  $\Lambda$ .** Features are always standardized to have mean 0 and standard deviation 1 in both linear and logistic regression, and the response is always centered to have mean 0 in linear regression. For lasso, the upper endpoint  $\lambda_{\max}$  of  $\Lambda = [\lambda_{\min}, \lambda_{\max}]$  is set to twice the maximum correlation between the features and response; that is,  $\lambda_{\max} = 2 \max_j |\frac{1}{n} \sum_{i=1}^n x_{ij} y_i|$ . For  $\ell_1$ -regularized logistic regression,  $\lambda_{\max} = 10 / \max_j |\frac{1}{n} \sum_{i=1}^n x_{ij} \tilde{y}_i|$  where  $\tilde{y}_i = y_i - \bar{y}(1 - \bar{y})$  and  $\bar{y} = \frac{1}{n} \sum_{i=1}^n y_i$ . Both constructions ensure all features have selection probability close to zero at  $\lambda_{\max}$ . For other regularized feature selection algorithms,  $\lambda_{\max}$  can be chosen via grid search.

Next, we define  $\lambda_{\min}$  by starting at  $\lambda = \lambda_{\max}$  and decreasing  $\lambda$  over a grid of 100 points that are evenly spaced on a log scale between  $\lambda_{\max}/10^{10}$  and  $\lambda_{\max}$ , stopping once  $\hat{S}_\lambda(\mathbf{Z}_{1:n})$  selects more than  $p/2$  features. We then set  $\lambda_0$  to be the smallest value of  $\lambda$  in this grid such that fewer than  $p/2$  features were selected. The idea is that we wish to quickly identify a reasonable lower endpoint that is not so close to  $\lambda_{\max}$  that the selection paths are cut off prematurely, but not so small that nearly all of the  $p$  features are selected, since exceedingly small regularization values can cause unnecessary computational difficulties. Our experience suggests that  $3p/4$  is an effective value for the maximum number of features selected and that results are insensitive to this choice.

Finally,  $\lambda_{\min}$  is chosen as follows. Given the integral cutoff value  $C > 0$ , recall that

$$\lambda_{\min} = \inf \{ \lambda \in (0, \lambda_{\max}) : \mathcal{I}(\lambda, \lambda_{\max}) \leq C \}$$

according to Equation 3.3 in the main text, where  $\mathcal{I}$  is an integral over  $[\lambda, \lambda_{\max}]$ . In practice, to approximate the infimum, we partition  $\Lambda = [\lambda_0, \lambda_{\max}]$  into a grid of  $r$  points evenly spaced on a log scale. We successively add the integrand of  $\mathcal{I}$  evaluated at each value of  $\lambda$  in the grid, starting from  $\lambda_{\max}$  and stopping either when  $\lambda = \lambda_0$  or when the sum surpasses  $C$ , whichever comes first. In the latter case,  $\lambda_{\min}$  is the smallest  $\lambda$  in the grid such that the corresponding Riemann sum in Proposition S1.1 is at most  $C$ .

**S1.2. Numerical approximation of the IPSS integral.** To implement IPSS, one must approximate the integral in Equation 3.1. We use a simple numerical approximation based on a Riemann sum, described in Proposition S1.1. Consider the class of probability measures  $\mu_\alpha(d\lambda) = z_\alpha^{-1} \lambda^{-\alpha} d\lambda$

on  $\Lambda = [\lambda_{\min}, \lambda_{\max}] \subseteq (0, \infty)$ , where  $\alpha \in \mathbb{R}$  and the normalizing constant  $z_\alpha$  is

$$z_\alpha = \int_{\Lambda} \lambda^{-\alpha} d\lambda = \begin{cases} \log(\lambda_{\max}/\lambda_{\min}) & \text{if } \alpha = 1 \\ \frac{1}{1-\alpha}(\lambda_{\max}^{1-\alpha} - \lambda_{\min}^{1-\alpha}) & \text{if } \alpha \neq 1. \end{cases}$$

The parameter  $\alpha$  controls the scale on which the  $\lambda$  values are weighted. For instance,  $\alpha = 0$  and  $\alpha = 1$  correspond to linear and log scales, respectively.

**Proposition S1.1.** *Fix  $\alpha \in \mathbb{R}$ , let  $\Lambda = [\lambda_{\min}, \lambda_{\max}] \subseteq (0, \infty)$ , and define  $\lambda_{k,r} = \lambda_{\min}^{1-k/r} \lambda_{\max}^{k/r}$  for all  $r \in \mathbb{N}$ ,  $k \in \{0, 1, \dots, r\}$ . For any Riemann integrable  $g : \Lambda \rightarrow \mathbb{R}$ ,*

$$\lim_{r \rightarrow \infty} \frac{1 - (\lambda_{\min}/\lambda_{\max})^{1/r}}{z_\alpha} \sum_{k=1}^r \lambda_{k,r}^{1-\alpha} g(\lambda_{k,r}) = \int_{\Lambda} g(\lambda) \mu_\alpha(d\lambda). \quad (\text{S1.1})$$

*Proof.* Fix  $m \in \mathbb{N}$ . The sequence  $\Lambda_r = (\lambda_{0,r}, \lambda_{1,r}, \dots, \lambda_{r,r})$  partitions  $\Lambda$ . Furthermore,

$$\lambda_{k,r} - \lambda_{k-1,r} = \left(1 - \left(\lambda_{\min}/\lambda_{\max}\right)^{1/r}\right) \lambda_{k,r} \quad (\text{S1.2})$$

for all  $r$  and  $k \in \{1, \dots, r\}$ , and hence,

$$\max_k |\lambda_{k,r} - \lambda_{k-1,r}| \leq \left|1 - \left(\lambda_{\min}/\lambda_{\max}\right)^{1/r}\right| |\lambda_{\max}| \rightarrow 0 \quad (\text{S1.3})$$

as  $r \rightarrow \infty$ . Therefore, Equations S1.2 and S1.3 imply that

$$\frac{1 - (\lambda_{\min}/\lambda_{\max})^{1/r}}{z_\alpha} \sum_{k=1}^r \lambda_{k,r}^{1-\alpha} g(\lambda_{k,r}) = \frac{1}{z_\alpha} \sum_{k=1}^r \lambda_{k,r}^{-\alpha} g(\lambda_{k,r})(\lambda_{k,r} - \lambda_{k-1,r}) \rightarrow \int_{\Lambda} g(\lambda) \mu_\alpha(d\lambda)$$

as  $r \rightarrow \infty$  since  $\lambda^{-\alpha} g(\lambda)$  is Riemann integrable on  $\Lambda$ .  $\square$

If  $\alpha = 1$  then  $\lambda_{k,r}^{1-\alpha} = 1$  for all  $k$  and  $r$ . Thus, when using  $f = h_m$  and  $\mu = \mu_1$  as in the main text, computation of the IPSS criterion (Equation 3.1) amounts to

$$\int_{\Lambda} f(\hat{\pi}_j(\lambda)) \mu(d\lambda) = \int_{\Lambda} h_m(\hat{\pi}_j(\lambda)) \mu_1(d\lambda) \approx \frac{1 - (\lambda_{\min}/\lambda_{\max})^{1/r}}{z_1} \sum_{k=1}^r h_m(\hat{\pi}_j(\lambda_{k,r})) \quad (\text{S1.4})$$

by applying Proposition S1.1 with  $\alpha = 1$  and  $g(\lambda) = h_m(\hat{\pi}_j(\lambda))$ . Furthermore,  $h_m$  is a simple function of the estimated selection probabilities, making Equation S1.4 very inexpensive to compute once the estimated selection probabilities are obtained.

The use of Proposition S1.1 for IPSS is justified by Proposition S1.2, which gives general conditions for functions of the form  $\lambda \mapsto f(\hat{\pi}_j(\lambda))$  to be Riemann integrable when  $\hat{S}_\lambda = \{j : \hat{\beta}_j(\lambda) \neq 0\}$  for some  $\hat{\beta}_j : \Lambda \rightarrow \mathbb{R}$ . In particular,  $h_m \circ \hat{\pi}_j$  is Riemann integrable when using lasso since  $h_m$  is continuous and lasso regularization paths  $\lambda \mapsto \hat{\beta}_j(\lambda)$  are continuous whenever no two features are perfectly correlated (Mairal and Yu, 2012). More generally, it follows from the proof of Proposition S1.2 that Riemann integrability of  $h_m \circ \hat{\pi}_j$  is implied by Riemann integrability of the indicators  $\mathbb{1}(j \in \hat{S}_\lambda)$ .

**Proposition S1.2.** *Let  $\Lambda$  be a closed interval in  $\mathbb{R}$ . Suppose  $\hat{S}_\lambda$  is given by  $\hat{S}_\lambda = \{j : \hat{\beta}_j(\lambda) \neq 0\}$  and that  $\lambda \mapsto \hat{\beta}_j(\lambda)$  is continuous on  $\Lambda$  for all  $j \in \{1, \dots, p\}$ . Then for every continuous function  $f : [0, 1] \rightarrow \mathbb{R}$ , the composition  $\lambda \mapsto f(\hat{\pi}_j(\lambda))$  is Riemann integrable.*

*Proof.* Fix  $j \in \{1, \dots, p\}$ . We first prove  $\lambda \mapsto \mathbf{1}(j \in \hat{S}_\lambda)$  is Riemann integrable. Since a bounded function on a closed interval is Riemann integrable if and only if it is continuous almost everywhere, it suffices to show  $\lambda \mapsto \mathbf{1}(j \in \hat{S}_\lambda)$  is continuous almost everywhere. To this end, we have

$$\mathbf{1}(j \in \hat{S}_\lambda) = \mathbf{1}(\hat{\beta}_j(\lambda) \neq 0) = \mathbf{1}(\lambda \in \hat{\beta}_j^{-1}(\mathbb{R} \setminus \{0\})).$$

Since  $\hat{\beta}_j$  is continuous,  $U = \hat{\beta}_j^{-1}(\mathbb{R} \setminus \{0\})$  is an open subset of  $\mathbb{R}$ . A classical result from analysis states that every open subset of  $\mathbb{R}$  is a countable union of disjoint open intervals. Letting  $U = \bigcup_{k=1}^{\infty} (a_k, b_k)$  be such a union, we have

$$\mathbf{1}(\lambda \in \hat{\beta}_j^{-1}(\mathbb{R} \setminus \{0\})) = \mathbf{1}(\lambda \in U) = \mathbf{1}(\lambda \in \bigcup_{k=1}^{\infty} (a_k, b_k)).$$

Hence,  $\mathbf{1}(j \in \hat{S}_\lambda) = \mathbf{1}(\lambda \in \bigcup_{k=1}^{\infty} (a_k, b_k))$ , and it is clear from the latter expression that the set of discontinuities of  $\mathbf{1}(j \in \hat{S}_\lambda)$  is contained in  $\bigcup_{k=1}^{\infty} \{a_k, b_k\}$ , which is countable and therefore has Lebesgue measure zero. Thus  $\lambda \mapsto \mathbf{1}(j \in \hat{S}_\lambda)$  is Riemann integrable, and it immediately follows that  $\hat{\pi}_j$  is Riemann integrable since it is a linear combination of indicators of the form  $\mathbf{1}(j \in \hat{S}_\lambda)$ .

To conclude the proof, we show that  $f \circ \hat{\pi}_j : \Lambda \rightarrow \mathbb{R}$  is bounded and continuous almost everywhere (and hence Riemann integrable). Boundedness holds because  $f$  is continuous on the compact set  $[0, 1]$ . For the continuous almost everywhere claim, let  $A$  and  $B$  be the sets of discontinuities of  $\hat{\pi}_j$  and  $f \circ \hat{\pi}_j$ , respectively. We know from the first part of the proof that  $A$  has measure zero. Thus, it suffices to show  $B \subseteq A$  or, equivalently,  $A^c \subseteq B^c$ . Fix  $\lambda \in A^c$  and let  $\lambda_k$  be any sequence in  $\Lambda$  converging to  $\lambda$ . Then  $y_k = \hat{\pi}_j(\lambda_k) \rightarrow \hat{\pi}_j(\lambda) = y$  since  $\hat{\pi}_j$  is continuous at  $\lambda$ . And since  $f$  is continuous,  $f(\hat{\pi}_j(\lambda_k)) = f(y_k) \rightarrow f(y) = f(\hat{\pi}_j(\lambda))$ . Thus  $\lambda \in B^c$  and hence  $A^c \subseteq B^c$ .  $\square$

---

## S2. PROOFS

---

We begin by introducing some notation and preliminary results. Fix  $B \geq 2$  throughout. For  $\lambda > 0$  and  $j \in \{1, \dots, p\}$ , define the *simultaneous selection probability*

$$\tilde{\pi}_j(\lambda) = \frac{1}{B} \sum_{b=1}^B \mathbf{1}(j \in \hat{S}_\lambda(\mathbf{Z}_{A_{2b-1}})) \mathbf{1}(j \in \hat{S}_\lambda(\mathbf{Z}_{A_{2b}})) = \frac{1}{B} \sum_{b=1}^B U_{jb}(\lambda)$$

where  $U_{jb}(\lambda) = \mathbf{1}(j \in \hat{S}_\lambda(\mathbf{Z}_{A_{2b-1}})) \mathbf{1}(j \in \hat{S}_\lambda(\mathbf{Z}_{A_{2b}}))$ . Here,  $\hat{S}_\lambda$  and  $A_{2b-1}, A_{2b}$  are defined as in Section 2.1. We use the following result (Equation S2.1), established in the proof of Lemma 1a of Shah and Samworth (2013): For all  $\lambda > 0$  and  $j \in \{1, \dots, p\}$ ,

$$\hat{\pi}_j(\lambda) \leq \frac{1}{2}(1 + \tilde{\pi}_j(\lambda)). \quad (\text{S2.1})$$

This holds since

$$0 \leq \frac{1}{B} \sum_{b=1}^B \left(1 - \mathbf{1}(j \in \hat{S}_\lambda(\mathbf{Z}_{A_{2b-1}}))\right) \left(1 - \mathbf{1}(j \in \hat{S}_\lambda(\mathbf{Z}_{A_{2b}}))\right) = 1 - 2\hat{\pi}_j(\lambda) + \tilde{\pi}_j(\lambda).$$

The following lemma is used in the proof of Theorem 4.1; it is essentially an application of the multinomial theorem. For readability, let us define  $\Delta_m = \{k \in \mathbb{Z}^B : k_1, \dots, k_B \geq 0, \sum_{b=1}^B k_b = m\}$ , denote the multinomial coefficients by

$$\binom{m}{k_1, \dots, k_B} = \frac{m!}{k_1! k_2! \dots k_B!},$$

and define  $N_k = \sum_{b=1}^B \mathbb{1}(k_b \neq 0)$  for  $k \in \Delta_m$ . Note that the assumed measurability of  $\hat{S}_\lambda(\mathbf{Z}_A) : \Lambda \times \Omega \rightarrow 2^{\{1, \dots, p\}}$  implies measurability of  $\tilde{\pi}_j$ ,  $\hat{\pi}_j$ , and any continuous functions thereof.

**Lemma S2.1.** *Fix  $m \in \mathbb{N}$ . If Condition 1 holds for all  $m' \in \{1, \dots, m\}$ , then for all  $\lambda > 0$ ,*

$$\max_{j \in S^c} \mathbb{E}(\tilde{\pi}_j(\lambda)^m) \leq \frac{1}{B^m} \sum_{k \in \Delta_m} \binom{m}{k_1, \dots, k_B} (q(\lambda)/p)^{2N_k}.$$

*Proof.* Fix  $j \in S^c$  and define  $0^0 = 1$ . By the multinomial theorem,

$$\begin{aligned} \tilde{\pi}_j(\lambda)^m &= \frac{1}{B^m} \left( \sum_{b=1}^B U_{jb}(\lambda) \right)^m = \frac{1}{B^m} \sum_{k \in \Delta_m} \binom{m}{k_1, \dots, k_B} \prod_{b=1}^B U_{jb}(\lambda)^{k_b} \\ &= \frac{1}{B^m} \sum_{k \in \Delta_m} \binom{m}{k_1, \dots, k_B} \prod_{b=1}^B U_{jb}(\lambda)^{\mathbb{1}(k_b \neq 0)}. \end{aligned}$$

The last equality holds because  $U_{jb}(\lambda) \in \{0, 1\}$ , and hence,  $U_{jb}(\lambda)^{k_b} = U_{jb}(\lambda)$  whenever  $k_b > 0$ . Next, since Condition 1 holds for all  $m' \leq m$  and since every  $k \in \Delta_m$  has at most  $m$  nonzero integers,

$$\mathbb{E} \prod_{b=1}^B U_{jb}(\lambda)^{\mathbb{1}(k_b \neq 0)} = \mathbb{P} \left( j \in \bigcap_{b: k_b \neq 0} (\hat{S}_\lambda(\mathbf{Z}_{A_{2b-1}}) \cap \hat{S}_\lambda(\mathbf{Z}_{A_{2b}})) \right) \leq (q(\lambda)/p)^{2N_k}.$$

Therefore,

$$\begin{aligned} \mathbb{E}(\tilde{\pi}_j(\lambda)^m) &= \frac{1}{B^m} \sum_{k \in \Delta_m} \binom{m}{k_1, \dots, k_B} \mathbb{E} \prod_{b=1}^B U_{jb}(\lambda)^{\mathbb{1}(k_b \neq 0)} \\ &\leq \frac{1}{B^m} \sum_{k \in \Delta_m} \binom{m}{k_1, \dots, k_B} (q(\lambda)/p)^{2N_k}. \end{aligned} \quad \square$$

**Proof of Theorem 4.1.** Fix  $\tau \in (0, 1]$  and  $m \in \mathbb{N}$ . Suppressing  $\lambda$  and  $\Lambda$  to declutter the notation,

$$\begin{aligned} \mathbb{P}(j \in \hat{S}_{\text{IPSS}, h_m}) &= \mathbb{P} \left( \int h_m(\hat{\pi}_j) d\mu \geq \tau \right) \leq \mathbb{P} \left( \int h_m \left( \frac{1}{2}(1 + \tilde{\pi}_j) \right) d\mu \geq \tau \right) = \mathbb{P} \left( \int \tilde{\pi}_j^m d\mu \geq \tau \right) \\ &\leq \frac{1}{\tau} \int \mathbb{E}(\tilde{\pi}_j^m) d\mu \leq \frac{1}{\tau B^m} \sum_{k \in \Delta_m} \binom{m}{k_1, \dots, k_B} \int (q/p)^{2N_k} d\mu \end{aligned} \quad (\text{S2.2})$$

for all  $j \in S^c$ . The first inequality holds by Equation S2.1, namely  $\hat{\pi}_j \leq \frac{1}{2}(1 + \tilde{\pi}_j)$ , and the fact that  $h_m$  is monotonically increasing. The second equality holds since by the definition of  $h_m$  in Equation 3.2,  $h_m(\frac{1}{2}(1 + x)) = x^m$  for  $x \in [0, 1]$ . The second inequality is Markov's inequality followed by exchanging the order of integration and expectation, which is justified by Tonelli's theorem since  $\tilde{\pi}_j(\lambda)^m$  is nonnegative and measurable. The last inequality holds by Lemma S2.1.

Thus,

$$\begin{aligned}
\mathbb{E}|\hat{S}_{\text{IPSS},h_m} \cap S^c| &= \mathbb{E} \sum_{j=1}^p \mathbb{1}(j \in \hat{S}_{\text{IPSS},h_m}) \mathbb{1}(j \in S^c) = \sum_{j=1}^p \mathbb{P}(j \in \hat{S}_{\text{IPSS},h_m}) \mathbb{1}(j \in S^c) \\
&\leq \frac{1}{\tau B^m} \sum_{k \in \Delta_m} \binom{m}{k_1, \dots, k_B} \int (q/p)^{2N_k} d\mu \sum_{j=1}^p \mathbb{1}(j \in S^c) \\
&\leq \frac{p}{\tau B^m} \sum_{k \in \Delta_m} \binom{m}{k_1, \dots, k_B} \int (q/p)^{2N_k} d\mu. \quad \square
\end{aligned}$$

**Proof of Theorem 4.2.** In the notation of this section, Equation 4.2 becomes

$$\mathbb{E}(\text{FP}) \leq \frac{p}{\tau B^m} \sum_{k \in \Delta_m} \binom{m}{k_1, \dots, k_B} \int (q/p)^{2N_k} d\mu$$

where  $q = q(\lambda)$ . When  $m = 1$ , each  $k \in \Delta_1$  has a single nonzero entry  $k_b = 1$ ; thus,  $|\Delta_1| = B$  and  $N_k = 1$  for all  $k \in \Delta_1$ . Therefore,

$$\mathbb{E}(\text{FP}) \leq \frac{p}{\tau B} \sum_{k \in \Delta_1} \binom{1}{k_1, \dots, k_B} \int (q/p)^{2N_k} d\mu = \frac{p}{\tau B} \sum_{b=1}^B \int (q/p)^2 d\mu = \frac{1}{\tau} \int \frac{q^2}{p} d\mu.$$

When  $m = 2$ , there are  $B$  elements  $k \in \Delta_2$  with  $N_k = 1$  (each of which has  $k_b = 2$  for exactly one  $b$ ), and  $\binom{B}{2}$  elements  $k \in \Delta_2$  with  $N_k = 2$  (each of which has  $k_b = k_{b'} = 1$  for some  $b \neq b'$ ). Therefore,

$$\mathbb{E}(\text{FP}) \leq \frac{p}{\tau B^2} \sum_{k \in \Delta_2} \binom{2}{k_1, \dots, k_B} \int (q/p)^{2N_k} d\mu = \frac{1}{\tau B^2} \int \left( \frac{Bq^2}{p} + \frac{B(B-1)q^4}{p^3} \right) d\mu.$$

When  $m = 3$ , there are  $B$  elements  $k \in \Delta_3$  with  $N_k = 1$  (each of which has  $k_b = 3$  for one  $b$ ), there are  $2\binom{B}{2}$  elements  $k \in \Delta_3$  with  $N_k = 2$  (having  $k_b = 2$  and  $k_{b'} = 1$  for some  $b \neq b'$ ), and  $\binom{B}{3}$  elements  $k \in \Delta_3$  with  $N_k = 3$  (having  $k_b = k_{b'} = k_{b''} = 1$  for some distinct  $b, b', b''$ ). Therefore,

$$\begin{aligned}
\mathbb{E}(\text{FP}) &\leq \frac{p}{\tau B^3} \sum_{k \in \Delta_3} \binom{3}{k_1, \dots, k_B} \int (q/p)^{2N_k} d\mu \\
&= \frac{1}{\tau B^3} \int \left( \frac{Bq^2}{p} + \frac{3B(B-1)q^4}{p^3} + \frac{B(B-1)(B-2)q^6}{p^5} \right) d\mu. \quad \square
\end{aligned}$$

---

### S3. IPSS WITH OTHER FUNCTIONS

---

In this section, we provide results about IPSS for other choices of  $f$ . Throughout, we fix  $\Lambda \subseteq (0, \infty)$  and a probability measure  $\mu$  on  $\Lambda$ .

Our first result says that if a function  $g$  dominates  $f$ , then the expected number of false positives selected by IPSS with  $f$  is at most the expected number of false positives selected by IPSS with  $g$ . Similarly, the expected number of false negatives for IPSS with  $g$  is at most the expected number of false negatives IPSS with  $f$ . We do not use Lemma S3.1 in this work, but it gives intuition for how IPSS depends on the choice of  $f$ , and could lead to useful bounds on functions not considered here.

**Lemma S3.1.** *Let  $f$  and  $g$  be functions from  $[0, 1]$  to  $\mathbb{R}$ . If  $f \leq g$  then for all  $\tau \in (0, 1]$ ,*

$$\mathbb{E}|\hat{S}_{\text{IPSS},f} \cap S^c| \leq \mathbb{E}|\hat{S}_{\text{IPSS},g} \cap S^c| \quad \text{and} \quad \mathbb{E}|\hat{S}_{\text{IPSS},g}^c \cap S| \leq \mathbb{E}|\hat{S}_{\text{IPSS},f}^c \cap S|.$$

*Proof.* Fix  $j \in \{1, \dots, p\}$  and  $\tau \in (0, 1]$ . Since  $f \leq g$ ,

$$\mathbb{P}(j \in \hat{S}_{\text{IPSS},f}) = \mathbb{P}\left(\int f(\hat{\pi}_j) d\mu \geq \tau\right) \leq \mathbb{P}\left(\int g(\hat{\pi}_j) d\mu \geq \tau\right) = \mathbb{P}(j \in \hat{S}_{\text{IPSS},g}).$$

Therefore,

$$\mathbb{E}|\hat{S}_{\text{IPSS},f} \cap S^c| = \sum_{j=1}^p \mathbb{P}(j \in \hat{S}_{\text{IPSS},f}) \mathbb{1}(j \in S^c) \leq \sum_{j=1}^p \mathbb{P}(j \in \hat{S}_{\text{IPSS},g}) \mathbb{1}(j \in S^c) = \mathbb{E}|\hat{S}_{\text{IPSS},g} \cap S^c|.$$

Similarly,

$$\begin{aligned} \mathbb{E}|\hat{S}_{\text{IPSS},g}^c \cap S| &= \sum_{j=1}^p \mathbb{P}(j \notin \hat{S}_{\text{IPSS},g}) \mathbb{1}(j \in S) = \sum_{j=1}^p (1 - \mathbb{P}(j \in \hat{S}_{\text{IPSS},g})) \mathbb{1}(j \in S) \\ &\leq \sum_{j=1}^p (1 - \mathbb{P}(j \in \hat{S}_{\text{IPSS},f})) \mathbb{1}(j \in S) = \mathbb{E}|\hat{S}_{\text{IPSS},f}^c \cap S|. \end{aligned} \quad \square$$

**S3.1. Functions defined by monomials.** The functions  $h_m$  defined in Equation 3.2 are zero on  $[0, 0.5]$ . Another natural class of functions  $\{w_m : m \in \mathbb{N}\}$  on  $[0, 1]$  is defined by

$$w_m(x) = x^m.$$

The  $w$  stands for “whole,” indicating that these functions are positive on the whole unit interval. For example, TIGRESS (Haury et al., 2012) uses a special case of IPSS with  $f = w_1$ ; see Section 2.3. Theorem S3.2 uses the following slight variation of Condition 1.

**Condition 2.** *We say Condition 2 holds for  $m$  if for all  $\lambda \in \Lambda$  and  $\mathcal{B} \subseteq \{1, \dots, 2B\}$  with  $|\mathcal{B}| = m$ ,*

$$\max_{j \in S^c} \mathbb{P}\left(j \in \bigcap_{b \in \mathcal{B}} \hat{S}_\lambda(\mathbf{Z}_{A_b})\right) \leq (q(\lambda)/p)^m.$$

**Theorem S3.2.** *Let  $\tau \in (0, 1]$  and  $m \in \mathbb{N}$ . If Condition 2 holds for all  $m' \in \{1, \dots, m\}$ , then*

$$\mathbb{E}|\hat{S}_{\text{IPSS},w_m} \cap S^c| \leq \frac{p}{\tau(2B)^m} \sum_{k_1 + \dots + k_{2B} = m} \binom{m}{k_1, \dots, k_{2B}} \int_{\Lambda} (q(\lambda)/p)^{\sum_{b=1}^{2B} \mathbb{1}(k_b \neq 0)} \mu(d\lambda)$$

where  $B$  is the number of subsampling steps in Algorithm 1 and the sum is over all nonnegative integers  $k_1, \dots, k_{2B}$  such that  $k_1 + \dots + k_{2B} = m$ .

While Theorems S3.2 and 4.1 appear similar, there are two key differences. First, Theorem S3.2 has an additional factor of  $2^m$  in the denominator, which is favorable in terms of tightness of the bound. On the other hand, the integrand in Theorem S3.2 is  $(q(\lambda)/p)^{N_k}$  rather than  $(q(\lambda)/p)^{2N_k}$  as in Theorem 4.1. Doubling the exponent makes the integral in Theorem 4.1 significantly smaller than the one in Theorem S3.2, since one typically has  $q(\lambda) \ll p$  over much of  $\Lambda$ . This advantage outweighs the countervailing factor of  $2^m$ , which is why we recommend using  $h_m$  in the main text.

*Proof of Theorem S3.2.* Fix  $\tau \in (0, 1]$  and  $m \in \mathbb{N}$ . The proof is almost exactly the same as that of Theorem 4.1. Specifically, suppressing  $\lambda$  and  $\Lambda$  from the notation, the multinomial theorem gives

$$\hat{\pi}_j^m = \left( \frac{1}{2B} \sum_{b=1}^{2B} \mathbb{1}(j \in \hat{S}_\lambda(\mathbf{Z}_{A_b})) \right)^m = \frac{1}{(2B)^m} \sum_{k_1+\dots+k_{2B}=m} \binom{m}{k_1, \dots, k_{2B}} \prod_{b: k_b \neq 0} \mathbb{1}(j \in \hat{S}_\lambda(\mathbf{Z}_{A_b})).$$

Since Condition 2 holds for all  $m' \leq m$  and since at most  $m$  of  $k_1, \dots, k_{2B}$  are nonzero,

$$\begin{aligned} \mathbb{E}(\hat{\pi}_j^m) &= \frac{1}{(2B)^m} \sum_{k_1+\dots+k_{2B}=m} \binom{m}{k_1, \dots, k_{2B}} \mathbb{E} \prod_{b: k_b \neq 0} \mathbb{1}(j \in \hat{S}_\lambda(\mathbf{Z}_{A_b})) \\ &\leq \frac{1}{(2B)^m} \sum_{k_1+\dots+k_{2B}=m} \binom{m}{k_1, \dots, k_{2B}} (q/p)^{N_k} \end{aligned}$$

where  $N_k = \sum_{b=1}^{2B} \mathbb{1}(k_b \neq 0)$ . So for any  $j \in \{1, \dots, p\}$ , Markov's inequality gives

$$\begin{aligned} \mathbb{P}(j \in \hat{S}_{\text{IPSS}, w_m}) &= \mathbb{P} \left( \int w_m(\hat{\pi}_j) d\mu \geq \tau \right) = \mathbb{P} \left( \int \hat{\pi}_j^m d\mu \geq \tau \right) \leq \frac{1}{\tau} \int \mathbb{E}(\hat{\pi}_j^m) d\mu \\ &\leq \frac{1}{\tau(2B)^m} \sum_{k_1+\dots+k_{2B}=m} \binom{m}{k_1, \dots, k_{2B}} \int (q/p)^{N_k} d\mu, \end{aligned}$$

where Tonelli's theorem justifies interchanging the order of expectation and integration. Therefore,

$$\begin{aligned} \mathbb{E}|\hat{S}_{\text{IPSS}, w_m} \cap S^c| &= \sum_{j=1}^p \mathbb{P}(j \in \hat{S}_{\text{IPSS}, w_m}) \mathbb{1}(j \in S^c) \\ &\leq \frac{1}{\tau(2B)^m} \sum_{k_1+\dots+k_{2B}=m} \binom{m}{k_1, \dots, k_{2B}} \int (q/p)^{N_k} d\mu \sum_{j=1}^p \mathbb{1}(j \in S^c) \\ &\leq \frac{p}{\tau(2B)^m} \sum_{k_1+\dots+k_{2B}=m} \binom{m}{k_1, \dots, k_{2B}} \int (q/p)^{N_k} d\mu. \end{aligned} \quad \square$$

**S3.2. Some piecewise linear functions.** For  $\delta \in [0, 1)$  define  $f_\delta : [0, 1] \rightarrow [0, 1]$  by

$$f_\delta(x) = \left( \frac{x - \delta}{1 - \delta} \right) \mathbb{1}(x \geq \delta).$$

Note that  $f_\delta$  is identically 0 on  $[0, \delta]$  and then rises linearly on  $[\delta, 1]$ . Theorem S3.3 is a continuous analogue of Theorem 1 from Meinshausen and Bühlmann (2010) when  $\delta = 0$ .

**Theorem S3.3.** Let  $\delta \in [0, 1)$ ,  $\tau \in (0, 1]$  such that  $\tau > \frac{1-2\delta}{2(1-\delta)}$ . If Condition 1 holds for  $m = 1$ , then

$$\mathbb{E}|\hat{S}_{\text{IPSS}, f_\delta} \cap S^c| \leq \frac{1}{2(\tau - \tau\delta + \delta) - 1} \int_{\Lambda} \frac{q(\lambda)^2}{p} \mu(d\lambda).$$

*Proof.* Let  $\delta \in [0, 1)$  and  $\tau \in (0, 1]$  such that  $\tau > (1 - 2\delta)/(2 - 2\delta)$ . Fix  $j \in S^c$ . We have

$$\begin{aligned}\mathbb{P}(j \in \hat{S}_{\text{IPSS}, f_\delta}) &= \mathbb{P}\left(\int f_\delta(\hat{\pi}_j) d\mu \geq \tau\right) \leq \mathbb{P}\left(\frac{1}{1-\delta} \int (\frac{1}{2}(1+\tilde{\pi}_j) - \delta) d\mu \geq \tau\right) \\ &= \mathbb{P}\left(\int \tilde{\pi}_j d\mu \geq 2(\tau - \delta\tau + \delta) - 1\right) \leq \frac{1}{2(\tau - \delta\tau + \delta) - 1} \int \mathbb{E}(\tilde{\pi}_j) d\mu \\ &\leq \frac{1}{2(\tau - \delta\tau + \delta) - 1} \int (q/p)^2 d\mu.\end{aligned}$$

The first inequality holds since  $f_\delta(\hat{\pi}_j) \leq f_\delta(\frac{1}{2}(1+\tilde{\pi}_j)) = (\frac{1}{2}(1+\tilde{\pi}_j) - \delta)/(1-\delta)$  by Equation S2.1 and because  $f_\delta$  is monotonically increasing with  $f_\delta(x) = (x-\delta)/(1-\delta)$  for  $x \geq 1/2$ . The second inequality is by Markov's inequality and Tonelli's theorem. The final inequality follows from the definition of  $\tilde{\pi}_j$  and the assumption that Condition 1 holds for  $m = 1$ . The assumption  $\tau > (1 - 2\delta)/(2 - 2\delta)$  implies  $2(\tau - \delta\tau + \delta) - 1 > 0$ , so the leading fraction is well-defined. Therefore,

$$\begin{aligned}\mathbb{E}|\hat{S}_{\text{IPSS}, f_\delta} \cap S^c| &= \mathbb{E}\left(\sum_{j=1}^p \mathbb{1}(j \in \hat{S}_{\text{IPSS}, f_\delta}) \mathbb{1}(j \in S^c)\right) = \sum_{j=1}^p \mathbb{P}(j \in \hat{S}_{\text{IPSS}, f_\delta}) \mathbb{1}(j \in S^c) \\ &\leq \frac{1}{2(\tau - \delta\tau + \delta) - 1} \int \frac{q^2}{p^2} d\mu \sum_{j=1}^p \mathbb{1}(j \in S^c) d\mu \leq \frac{1}{2(\tau - \delta\tau + \delta) - 1} \int \frac{q^2}{p} d\mu. \quad \square\end{aligned}$$

---

#### S4. IPSS WITH OTHER BASE ESTIMATORS

---

IPSS can be used with any base estimator  $\hat{S}_\lambda$  that performs feature selection and depends upon a parameter  $\lambda \in \mathbb{R}$ . Not all methods can be used, however. One such example is the debiased lasso, a popular approach for producing an unbiased estimator  $\hat{\beta}_u$  of the true coefficient vector  $\beta^*$  in the linear model  $Y = X^\top \beta^* + \epsilon$  (Javanmard and Montanari, 2014). Given observations  $(\mathbf{x}_i, y_i)$  of  $n$  random vectors  $(\mathbf{X}_i, Y_i)$  and a regularization value  $\lambda > 0$ , this estimator takes the form

$$\hat{\beta}_u(\lambda) = \hat{\beta}(\lambda) + \frac{1}{n} M \mathbf{X}^\top (\mathbf{Y} - \mathbf{X} \hat{\beta}(\lambda))$$

where  $\mathbf{X} \in \mathbb{R}^{n \times p}$  is the design matrix,  $\mathbf{Y} = (y_1, \dots, y_n)^\top$ ,  $\hat{\beta}(\lambda)$  is the lasso solution (Equation 2.1), and  $M \in \mathbb{R}^{p \times p}$  is the solution of a certain convex program (Javanmard and Montanari, 2014). The problem with respect to IPSS is that every entry of the correction term  $M \mathbf{X}^\top (\mathbf{Y} - \mathbf{X} \hat{\beta}(\lambda))$  is usually nonzero, even for features  $X_j$  with  $\beta_j^* = 0$ . Consequently, all entries of  $\hat{\beta}_u(\lambda)$  are nonzero and hence  $\hat{S}_\lambda = \{j : \hat{\beta}_u(\lambda) \neq 0\} = \{1, \dots, p\}$ . Thus, unlike lasso, whose solutions typically include zeros, the debiased lasso does not inherently perform feature selection in the finite sample setting, making it incompatible with IPSS and stability selection.

A general class of estimators in the linear regression setting that perform feature selection and are therefore compatible with IPSS is

$$\hat{\beta}_\varphi(\lambda) = \arg \min_{\beta \in \mathbb{R}^p} \frac{1}{2} \sum_{i=1}^n (y_i - \mathbf{x}_i^\top \beta)^2 + \sum_{j=1}^p \varphi(|\beta_j|, \lambda), \quad (\text{S4.1})$$

where  $\varphi$  is a penalty function. We consider three estimators based on Equation S4.1. First, lasso is the case of  $\varphi(x, \lambda) = \lambda x$  (Tibshirani, 1996), which we implement using the `scikit-learn` Python

package (Pedregosa et al., 2011). Second, the smoothly clipped absolute deviation penalty (SCAD), introduced by Fan and Li (2001), is

$$\varphi_{\text{SCAD}}(x, \lambda) = \begin{cases} \lambda|x| & \text{if } |x| \leq \lambda, \\ \frac{2\gamma\lambda|x| - x^2 - \lambda^2}{2(\gamma - 1)} & \text{if } \lambda < |x| \leq \gamma\lambda, \\ \frac{\lambda^2(\gamma + 1)}{2} & \text{if } |x| > \gamma\lambda. \end{cases}$$

Following Fan and Li (2001), we use  $\gamma = 3.7$  in all our experiments. Given  $\gamma$ , the solution  $\hat{\beta}_{\varphi_{\text{SCAD}}}(\lambda)$  to Equation S4.1 depends only on  $\lambda$  and can be used as a base estimator for IPSS.

Third, the minimax concave penalty, MCP (Zhang, 2010), is another case of Equation S4.1 where

$$\varphi_{\text{MCP}}(x, \lambda) = \begin{cases} \lambda|x| - \frac{x^2}{2\gamma} & \text{if } |x| \leq \gamma\lambda, \\ \frac{\gamma\lambda^2}{2} & \text{if } |x| > \gamma\lambda. \end{cases}$$

We use  $\gamma = 3$  in all our experiments, which is the default setting in the Python package `skglm` that we use to implement both MCP and SCAD (Bertrand et al., 2022). As with SCAD, once  $\gamma$  is fixed, the resulting MCP estimator can be used with IPSS.

In addition to the three estimators based on Equation S4.1, we consider IPSS with the adaptive lasso as the base estimator (Zou, 2006). In this case, the estimated coefficient vector is

$$\hat{\beta}_{\text{adap}} = \arg \min_{\beta \in \mathbb{R}^p} \frac{1}{2} \sum_{i=1}^n (y_i - \mathbf{x}_i^T \beta)^2 + \lambda \sum_{j=1}^p \hat{w}_j |\beta_j|,$$

where  $\hat{w}_j$  are data-dependent weights that modulate the regularization applied to each coefficient. Following Zou (2006), we set  $\hat{w}_j = 1/|\tilde{\beta}_j|$  where  $\tilde{\beta}$  is the solution to the ridge regression problem (Hoerl and Kennard, 1970), computed using the default settings in `scikit-learn` (Pedregosa et al., 2011). We use ridge regression to compute  $\tilde{\beta}$  since ordinary least squares is not applicable when  $p > n$ , as is the case in our simulations.

Finally, the optimization problem for  $\ell_1$ -regularized logistic regression is

$$\hat{\beta}(\lambda) = \arg \min_{\beta \in \mathbb{R}^p} - \sum_{i=1}^n [y_i \log(p_i) + (1 - y_i) \log(1 - p_i)] + \lambda \sum_{j=1}^p |\beta_j|, \quad (\text{S4.2})$$

where  $p_i = 1/(1 + \exp(-\mathbf{x}_i^T \beta))$  (Friedman et al., 2010). Here, the response variables  $Y_i$  take values in  $\{0, 1\}$ . Like lasso, the  $\ell_1$ -penalty in Equation S4.2 typically shrinks some entries of  $\hat{\beta}(\lambda)$  to zero, making  $\ell_1$ -regularized logistic regression compatible with IPSS.

---

## S5. EMPIRICAL STUDY OF THE THEORETICAL CONDITIONS

---

Our theory is based on Condition 1, which is less stringent than the exchangeability and not-worse-than-random-guessing conditions of Meinshausen and Bühlmann (2010); we refer to these as the MB conditions for short. However, Condition 1 does not hold in general. For example, these conditions tend to be violated when true and non-true features are highly correlated. Nonetheless, even then, empirically we find that only a small proportion of non-true features violate Condition 1 within

the interval  $[\lambda_{\min}, \lambda_{\max}]$ ; see Figure S1. This also illustrates how our construction of  $\lambda_{\min}$  prevents IPSS from integrating over small regularization values where Condition 1 tends to fail.

Additionally, in Figure S1 we see that for any given value of  $\lambda$ , Condition 1 tends to be more likely to hold as  $m$  increases. This subtle point contributes to the improved performance of IPSS relative to stability selection. Recall that the MB conditions imply Condition 1 when  $m = 1$ . Hence, for any given  $\lambda$ , the more frequent violations of Condition 1 when  $m = 1$  imply that the MB conditions are more frequently violated, compared to Condition 1 for  $m \in \{2, 3\}$ . Furthermore, while Equations 4.4 and 4.5 require Condition 1 to hold for  $m \in \{1, 2\}$  and  $m \in \{1, 2, 3\}$ , respectively, the  $1/B$  and  $1/B^2$  terms in their integrands mitigate the higher proportion of failures of Condition 1. This partly explains why the target  $E(\text{FP})$  is relatively well-approximated in all of our simulation results, even when Condition 1 does not necessarily hold for all features.

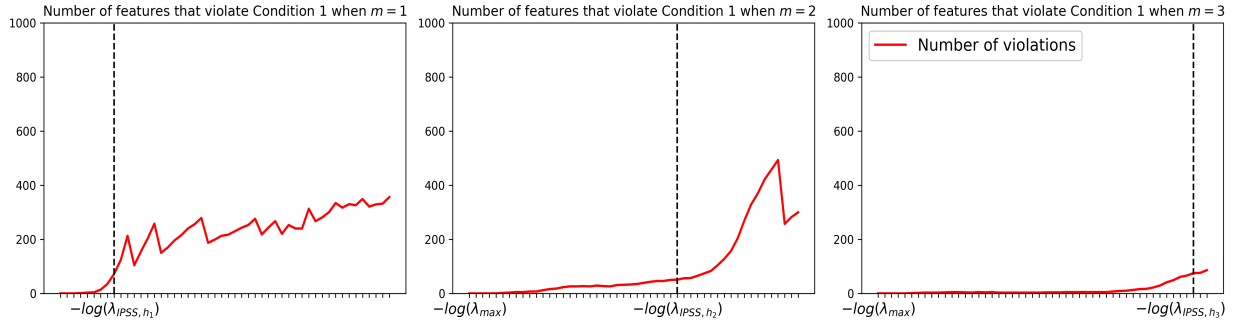


FIGURE S1. *Violations of Condition 1 for highly correlated data.* (Left) Number of features that violate Condition 1 when  $m = 1$  for each value of  $\lambda$ . (Middle, Right) Same as the left plot but for  $m = 2$  and 3. The dashed lines show  $-\log(\lambda_{\text{IPSS}, h_m})$ , where  $\lambda_{\text{IPSS}, h_m}$  is the  $\lambda_{\min}$  for IPSS with  $h_m$ . The horizontal axis, shown on a log scale, is the same in all three plots. Data are simulated from a linear regression model with normal residuals and Toeplitz design with  $\rho = 0.9$  (Section 5), with  $n = 200$ ,  $p = 1000$ ,  $s = 20$ , and SNR = 1.

---

## S6. ADDITIONAL APPLICATION RESULTS

---

Table S1 lists all of the proteins that are identified by the IPSS and stability selection methods in our prostate cancer RPPA study in Section 6.1. A  $\checkmark$  indicates that the protein was selected by the corresponding method, and an  $\times$  indicates that it was not selected. The references next to each protein provide further evidence that these proteins are related to prostate cancer. Table S2 is similar to Table S1, but for the colon cancer study in Section 6.2.

Protein	IPSS(cubic)	IPSS(quad)	r-concave	UM	MB
BAK1 (Shi et al., 2007)	✓	✗	✗	✗	✗
DIRAS3 (Sutton et al., 2019)	✓	✓	✓	✓	✓
MAPK9 (Rodríguez-Berriguete et al., 2012)	✓	✓	✓	✓	✓
STK11 (Grossi et al., 2015)	✓	✓	✗	✗	✗
NOTCH1 (Rice et al., 2019)	✓	✓	✓	✓	✓
PKC (Tanaka et al., 2003)	✓	✓	✗	✗	✗
PTEN (Jamaspishvili et al., 2018)	✓	✗	✗	✗	✗
SMAD1 (Qiu et al., 2007)	✓	✓	✗	✗	✗
EIF4E (D'Abrozo and Ghosh, 2018)	✓	✓	✓	✓	✓
SQSTM1 (Huang et al., 2018)	✓	✓	✓	✗	✗

TABLE S1. *Selected proteins from the prostate cancer RPPA data set.*

Gene	IPSS(cubic)	IPSS(quad)	r-concave	UM	None
R87126 (Wang et al., 2010)	✓	✓	✓	✓	✓
M63391 (Arentz et al., 2011)	✓	✓	✓	✓	✗
H08393 (Wang et al., 2010)	✓	✓	✓	✗	✗
Z50753 (Nomiri et al., 2022)	✓	✓	✓	✗	✗
J02854 (Wang et al., 2010)	✓	✓	✓	✗	✗
M26383 (Wang et al., 2010)	✓	✓	✓	✗	✗
H06524 (Chen et al., 2017)	✓	✓	✗	✗	✗
X12671 (Ushigome et al., 2005)	✓	✓	✓	✗	✗
R54097 (Zhang et al., 2020)	✓	✗	✗	✗	✗
X63629 (Sun et al., 2011)	✓	✓	✗	✗	✗
T62947 (Wang et al., 2006)	✓	✗	✗	✗	✗
M36634 (Levy et al., 2002)	✓	✓	✗	✗	✗
T92451 (Liu et al., 2009)	✓	✗	✗	✗	✗
T47377 (Wang et al., 2010)	✓	✗	✗	✗	✗
R36977 (Anuraga et al., 2021)	✓	✓	✗	✗	✗
H20709 (Liu et al., 2009)	✓	✗	✗	✗	✗

TABLE S2. *Selected genes from the colon cancer genomics data set.* Genes are identified by their GenBank accession numbers; here is a list of some of their official symbols (in parentheses): J02854 (MYL9), M26383 (IL-1), T47377 (S-100), J02854 (MYL9), M26383 (CXCL8), M36634 (VIP), M63391 (desmin), R36977 (GTF3A), R54097 (EIF2S2), X12671 (hnRNP A1), X63629 (P-cadherin), Z50753 (GUCA2B).

---

## S7. ADDITIONAL SIMULATION RESULTS

---

All results in this section are from the simulation experiments described in Section 5 of the main text. Figures S2 and S3 show results for linear regression for Student's  $t$  residuals with 2 degrees of freedom, Figures S4 and S5 show results for linear regression with normal residuals when the base estimator is MCP, Figures S6 and S7 show results for linear regression with normal residuals when the base estimator is SCAD, Figures S8 and S9 show results for linear regression with normal residuals when the base estimator is adaptive lasso, and Figures S10 and S11 show results for logistic regression when the base estimator is  $\ell_1$ -regularized logistic regression. In all cases, the same base estimator and stability paths are used for each of the IPSS and stability selection methods, and the IPSS parameters are always set to their default values, as described in Section S8.2.

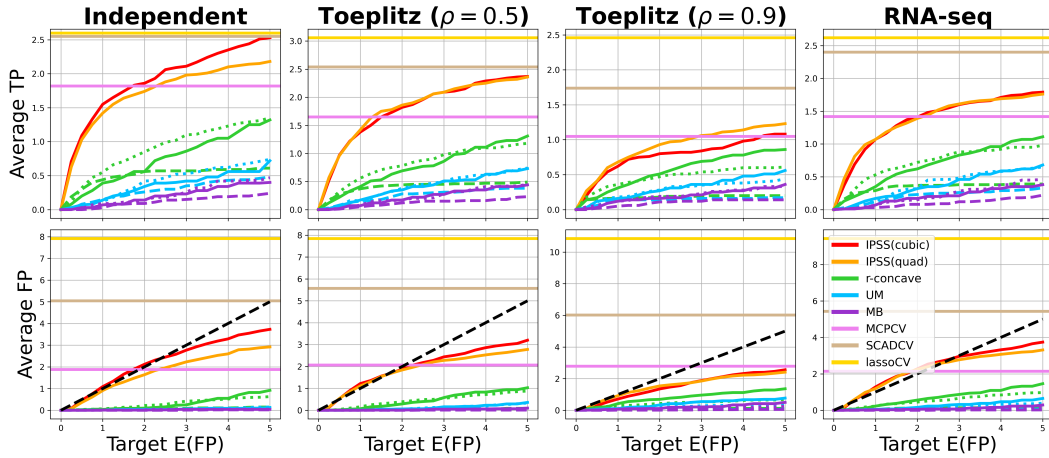


FIGURE S2. *Linear regression, Student's  $t$  residuals: Lasso ( $p = 200$ )*. The solid, dotted, and dashed lines for the stability selection methods represent  $\tau = 0.6, 0.75$ , and  $0.9$ , respectively. Cross-validation results (horizontal lines) are independent of Target E(FP). The dashed black line represents perfect E(FP) control.

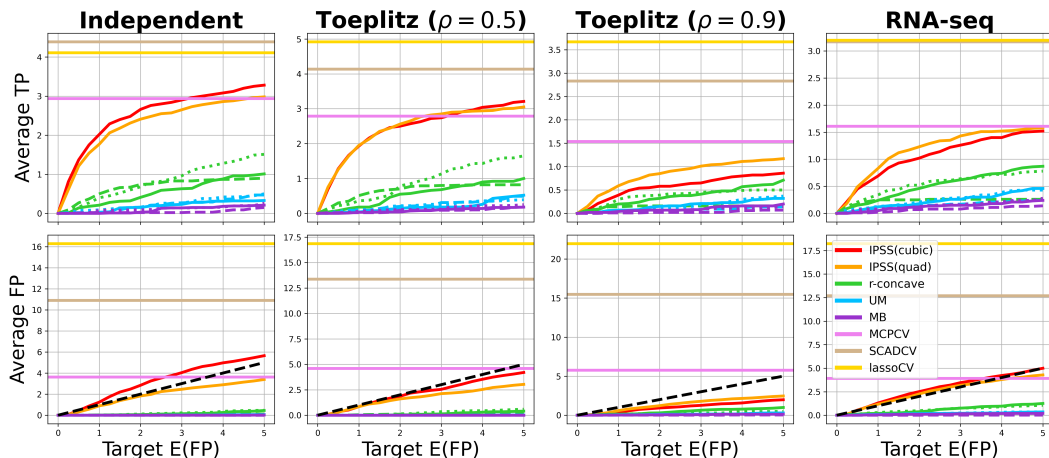


FIGURE S3. *Linear regression, Student's  $t$  residuals: Lasso ( $p = 1000$ )*. See Figure S2.

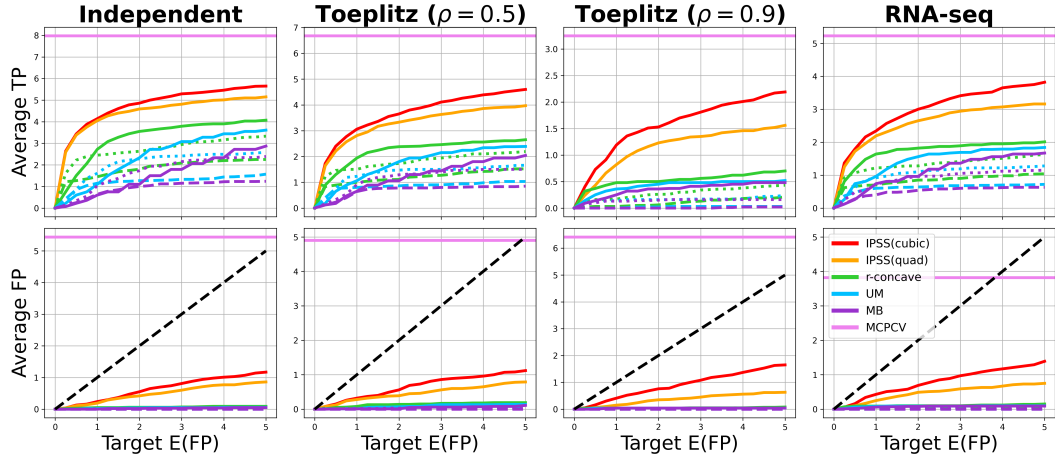


FIGURE S4. *Linear regression, normal residuals: MCP ( $p = 200$ )*. See Figure S2.

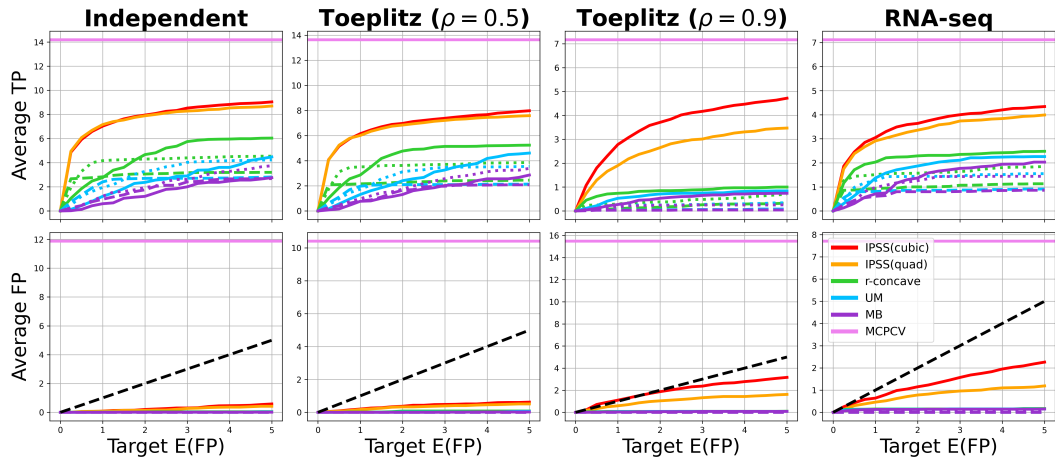


FIGURE S5. *Linear regression, normal residuals: MCP ( $p = 1000$ )*. See Figure S2.

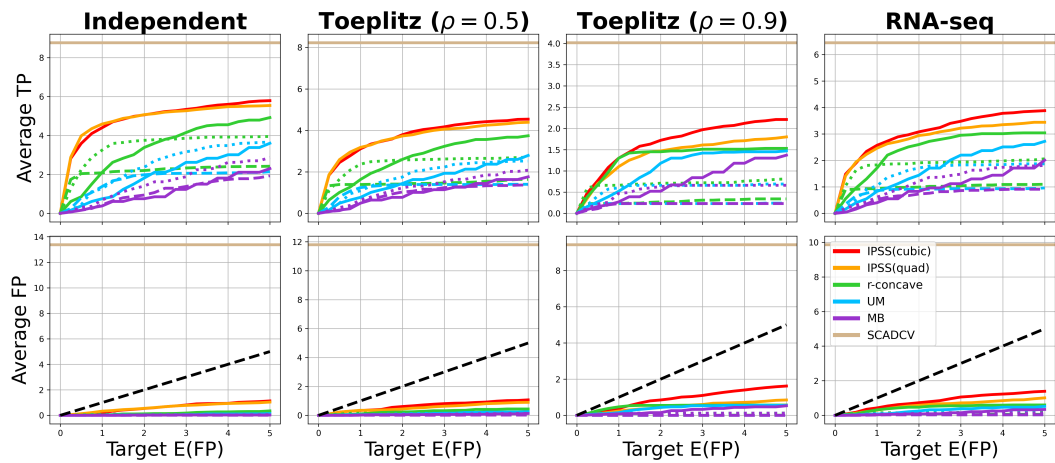


FIGURE S6. *Linear regression, normal residuals: SCAD ( $p = 200$ )*. See Figure S2.

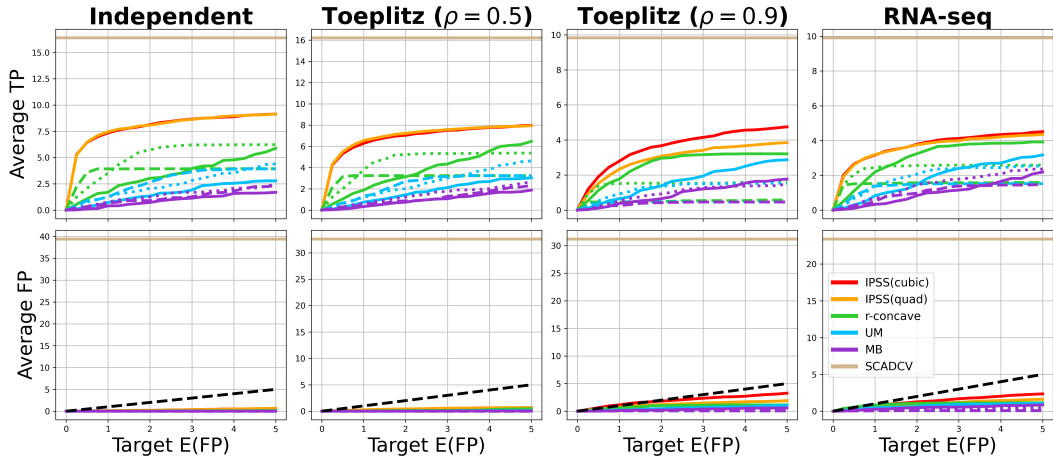


FIGURE S7. *Linear regression, normal residuals: SCAD ( $p = 1000$ )*. See Figure S2.

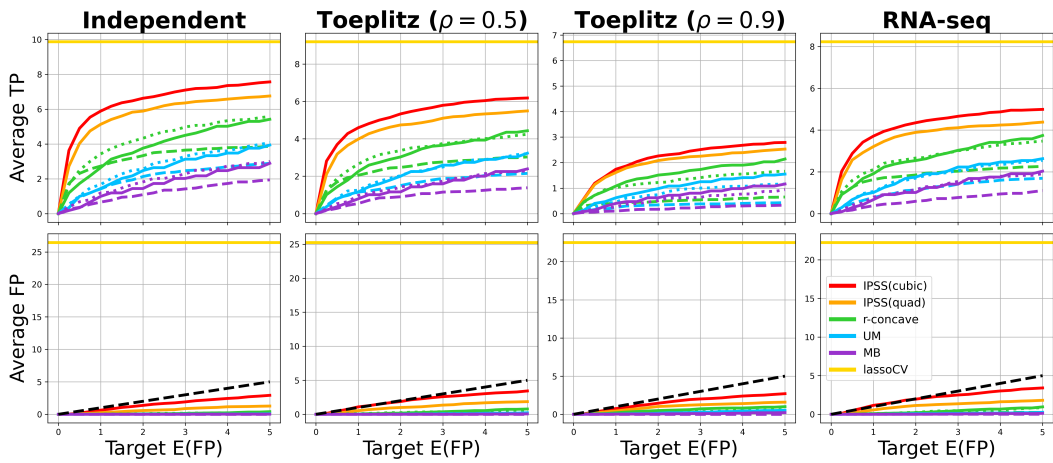


FIGURE S8. *Linear regression, normal residuals: Adaptive lasso ( $p = 200$ )*. See Figure S2.

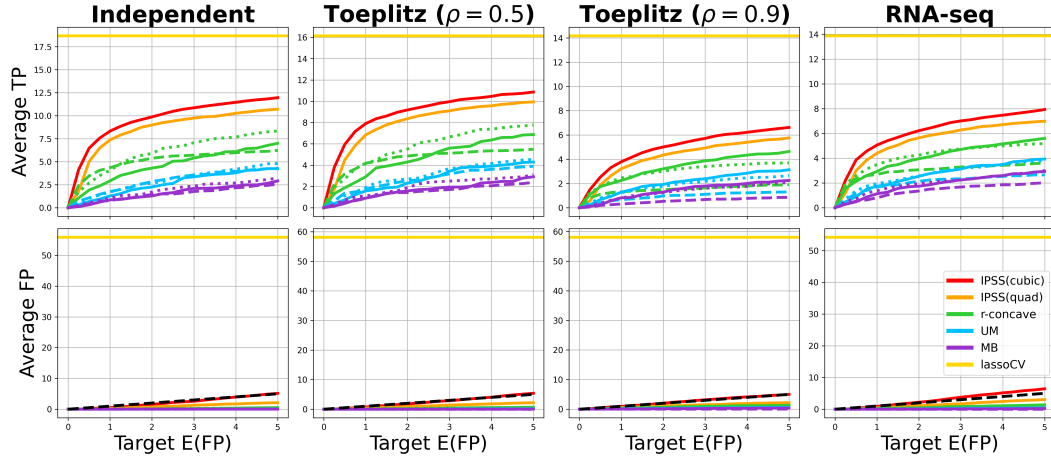


FIGURE S9. *Linear regression, normal residuals: Adaptive lasso ( $p = 1000$ )*. See Figure S2.

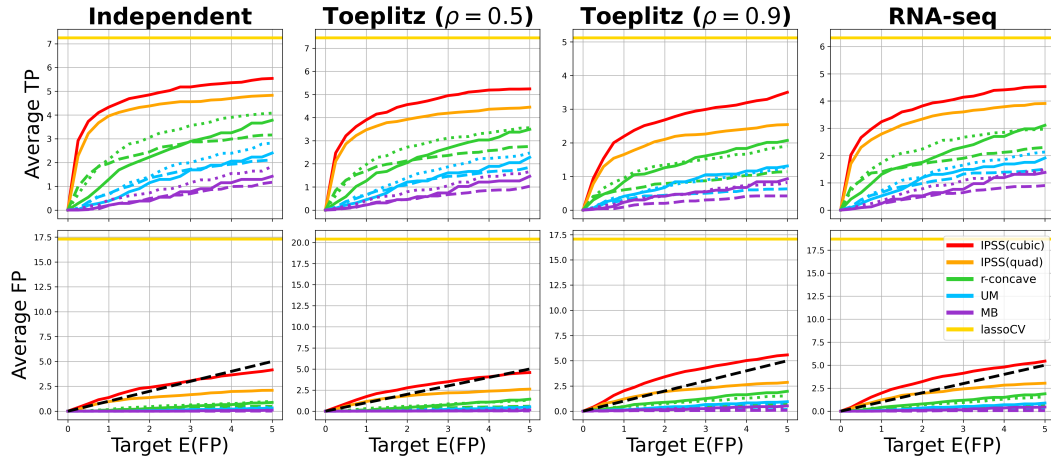


FIGURE S10.  $\ell_1$ -regularized logistic regression ( $p = 200$ ). See Figure S2.

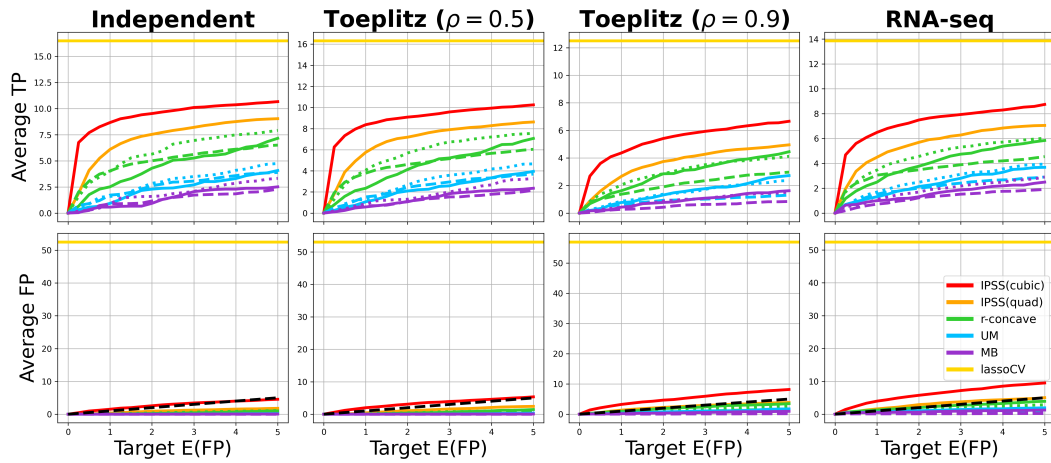


FIGURE S11.  $\ell_1$ -regularized logistic regression ( $p = 1000$ ). See Figure S2.

---

## S8. SENSITIVITY TO PARAMETERS

---

We assess the sensitivity of IPSS to the integral cutoff  $C$  (Section S8.1) and to the parameter  $\alpha$  that defines the probability measure  $\mu_\alpha \propto \lambda^{-\alpha} d\lambda$  (Section S8.2).

**S8.1. Sensitivity to  $C$ .** We ran IPSS(quad) and IPSS(cubic) with  $C \in \{0.025, 0.05, 0.75, 0.1\}$  for linear regression with normal residuals and logistic regression and for each feature design described in Section 5. Results are reported for lasso, MCP, SCAD, and  $\ell_1$ -regularized logistic regression. The  $\alpha$  parameter in  $\mu_\alpha$  is always set to the default values described in Section 5. In each plot, different colors correspond to different choices of  $C$ , and the solid and dashed lines correspond to IPSS(quad) and IPSS(cubic), respectively. The solid, dashed, and dotted gray curves—included for reference—correspond to MB, UM, and  $r$ -concave, respectively, each with  $\tau = 0.75$ .

The results in Figures S12 through S19 show that IPSS is highly robust to  $C$ , with different choices of  $C$  often yielding nearly indistinguishable solutions. This is because  $C$  directly determines  $\lambda_{\min}$  and, for the range of cutoffs we consider, the corresponding  $\lambda_{\min}$  values are sufficiently small that the stability paths are no longer changing in a meaningful way at these points, especially relative to the changes that occur at much larger regularization values (Figure 2). Thus, perturbations to  $C$  on the scale we consider do not meaningfully alter the stability paths and therefore the IPSS results.

**S8.2. Sensitivity to  $\alpha$ .** We ran IPSS(quad) and IPSS(cubic) for  $\alpha \in \{0, 1/4, 1/2, 3/4, 1, 5/4\}$  for linear regression with normal residuals and logistic regression and for each feature design described in Section 5. Results are reported for lasso, MCP, SCAD, and  $\ell_1$ -regularized logistic regression. The cutoff  $C$  is always set to 0.05. In each plot, different colors correspond to different choices of  $\alpha$ , and the solid and dashed lines correspond to IPSS(quad) and IPSS(cubic), respectively. The solid, dashed, and dotted gray curves—included for reference—correspond to MB, UM, and  $r$ -concave, respectively, each with  $\tau = 0.75$ .

The results in Figures S20 through S27 show that IPSS is robust to  $\alpha$  in general, with all choices of  $\alpha$  leading to more true positives than the stability selection methods, and most choices of  $\alpha$  producing accurate E(FP) control in most settings. There are two notable exceptions. First, both IPSS methods significantly exceed the target E(FP) when  $\alpha = 5/4$  in the  $p = 1000$  linear regression experiments with lasso as the base estimator. This issue—included here for illustrative purposes and easily avoided by simply not using  $\alpha = 5/4$  when the base estimator is lasso—occurs because  $\alpha = 5/4$  puts too much weight on small regularization values, leading to violations of Condition 1. The second notable exception is the  $p = 1000$  logistic regression experiments, where IPSS(cubic) with  $\alpha \in \{3/4, 1, 5/4\}$  and, to a lesser extent, IPSS(quad) with  $\alpha = 5/4$  significantly violate of the E(FP) bound. However, the remaining IPSS and  $\alpha$  combinations typically keep the actual E(FP) close to or below target levels.

While  $\alpha = 1$  works well in general, further improvements in performance are possible with other choices of  $\alpha$ . Based on our experience, we recommend  $\alpha = 5/4$  when MCP or SCAD are the base estimators. For IPSS with lasso or adaptive lasso as a base estimator, we recommend  $\alpha = 1$  if  $p \leq 200$ ,  $\alpha = 3/4$  if  $p \geq 1000$ , and  $\alpha = -\frac{p}{3200} + \frac{17}{16}$  for  $p \in (200, 1000)$ . The latter linearly interpolates between  $(p, \alpha) = (200, 1)$  and  $(1000, 3/4)$ . For IPSS with  $\ell_1$ -regularized logistic regression, we recommend  $\alpha = 1$  if  $p \leq 200$ ,  $\alpha = 0$  if  $p \geq 1000$ , and  $\alpha = -\frac{p}{800} + \frac{5}{4}$  for  $p \in (200, 1000)$ . The latter linearly interpolates between  $(p, \alpha) = (200, 1)$  and  $(1000, 0)$ .

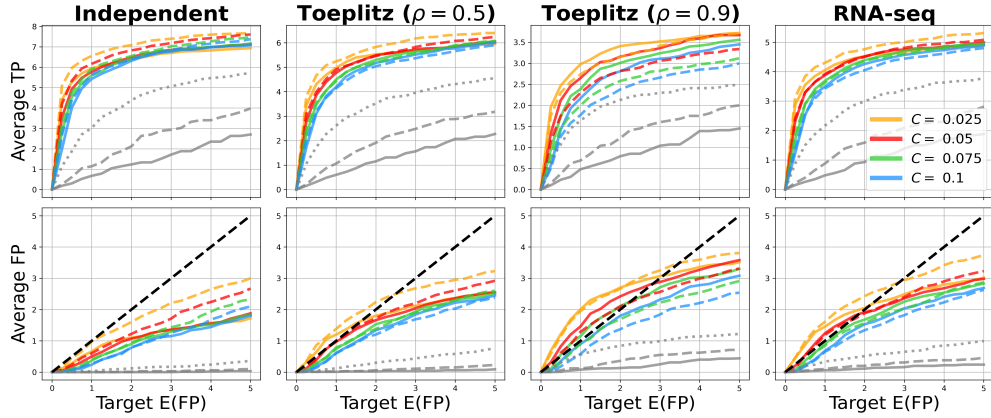


FIGURE S12. *Sensitivity to C: Lasso ( $p = 200$ )*. Colored solid and dashed curves show IPSS(quad) and IPSS(cubic) for different choices of  $C$ , respectively. Gray solid, dashed, and dotted gray curves show MB, UM, and  $r$ -concave stability selection with  $\tau = 0.75$ . The dashed black line represents perfect  $E(FP)$  control.

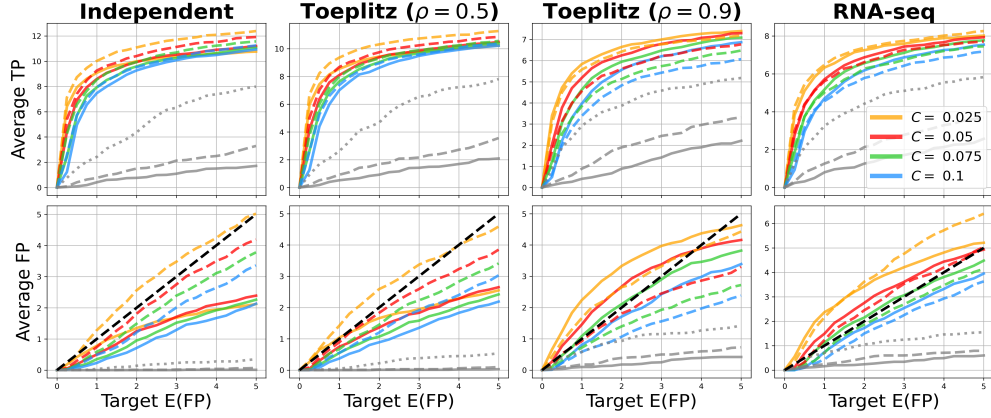


FIGURE S13. *Sensitivity to C: Lasso ( $p = 1000$ )*. See Figure S12.

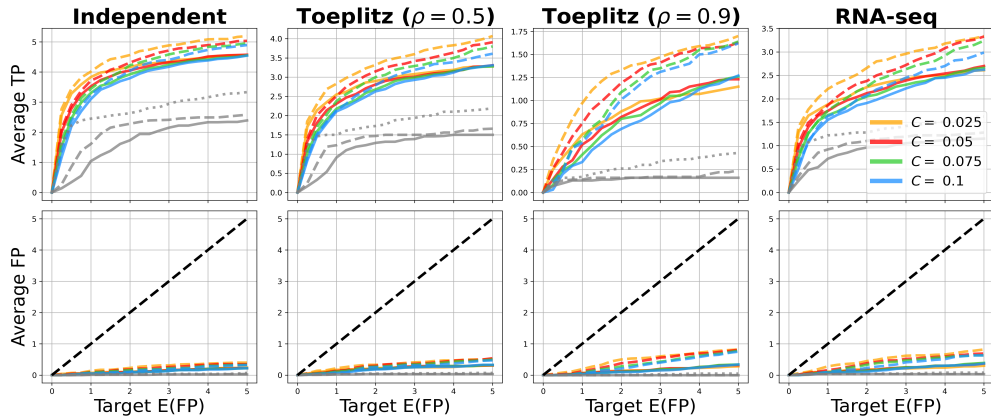


FIGURE S14. *Sensitivity to C: MCP ( $p = 200$ )*. See Figure S12.

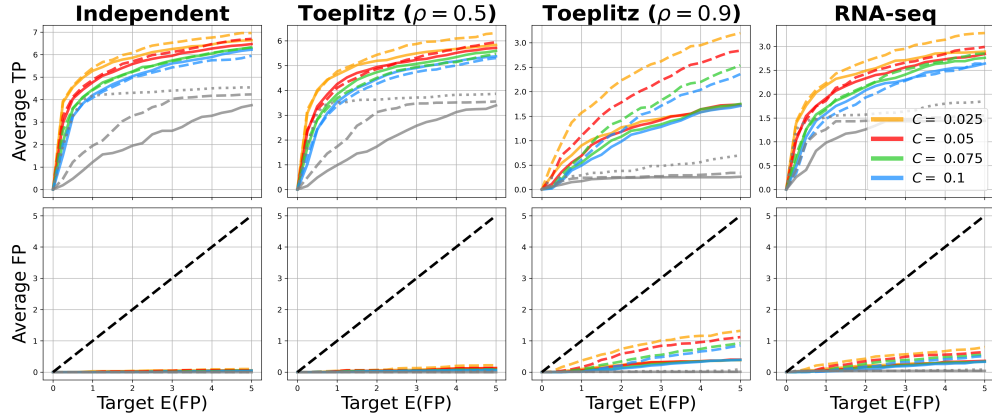


FIGURE S15. *Sensitivity to C: MCP ( $p = 1000$ )*. See Figure S12.

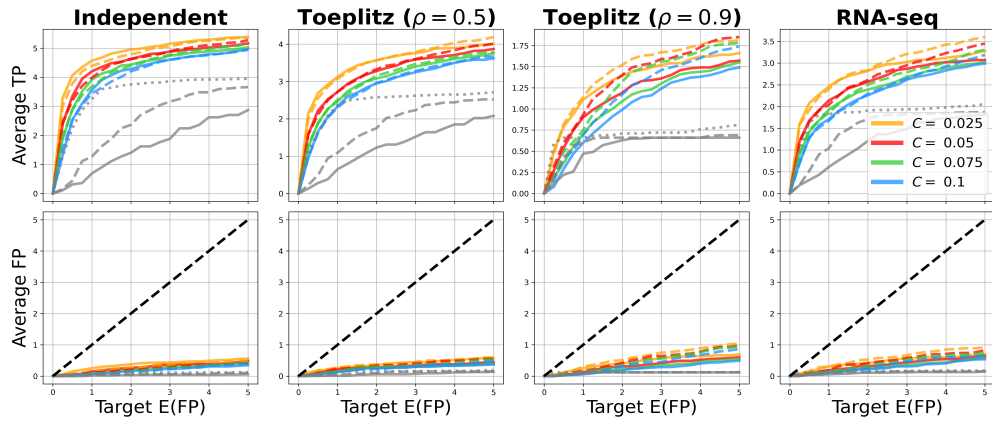


FIGURE S16. *Sensitivity to C: SCAD ( $p = 200$ )*. See Figure S12.

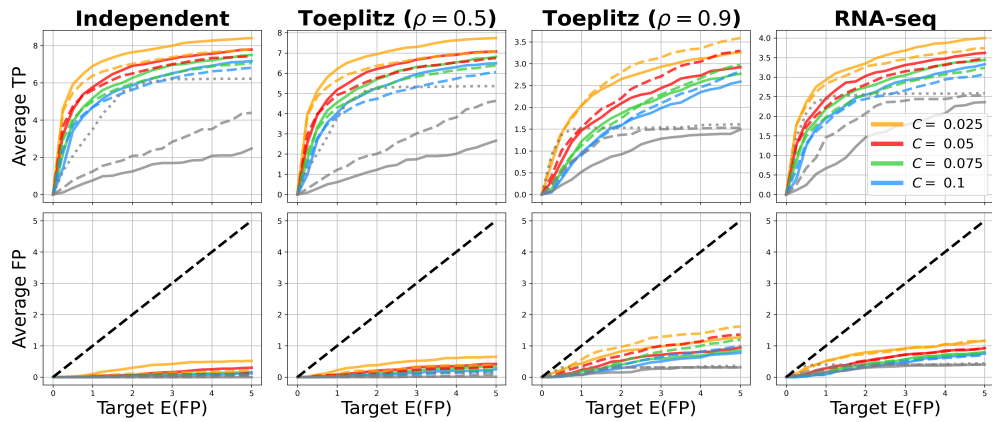


FIGURE S17. *Sensitivity to C: SCAD ( $p = 1000$ )*. See Figure S12.

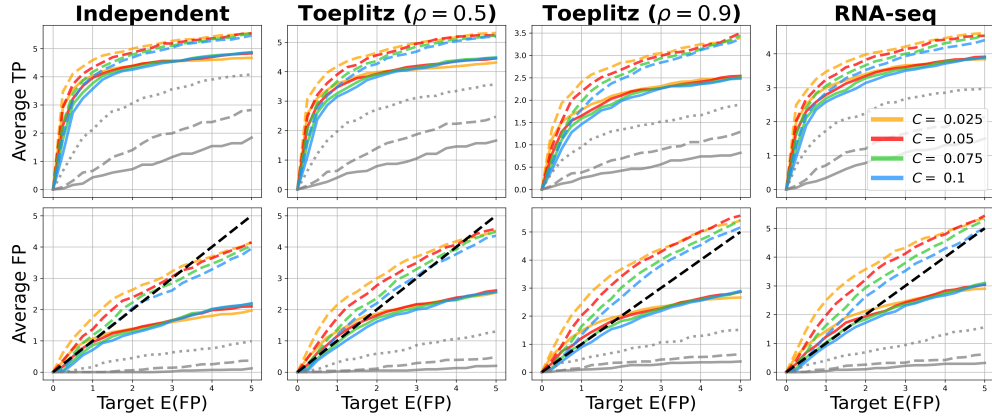


FIGURE S18. *Sensitivity to C: Logistic regression ( $p = 200$ )*. See Figure S12.

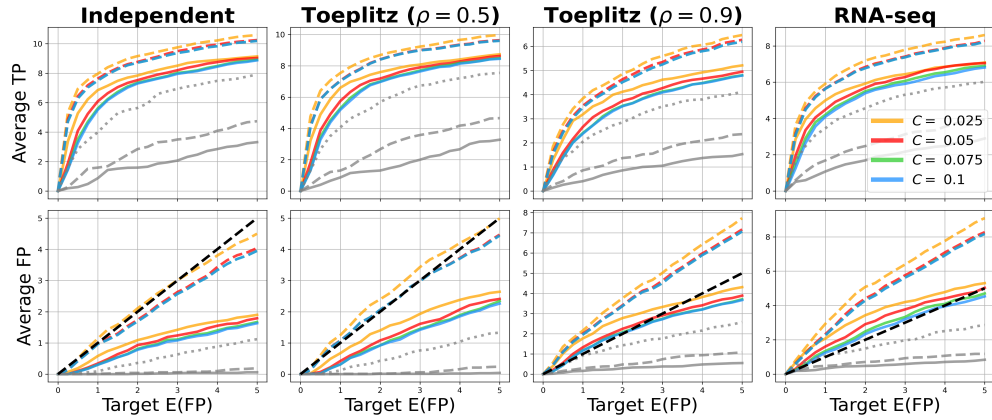


FIGURE S19. *Sensitivity to C: Logistic regression ( $p = 1000$ )*. See Figure S12.

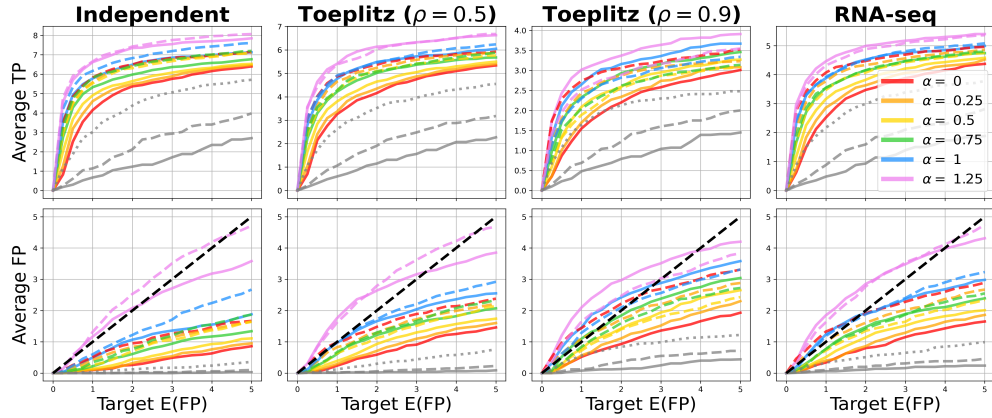


FIGURE S20. *Sensitivity to \alpha: Lasso ( $p = 200$ )*. Colored solid and dashed curves show IPSS(quad) and IPSS(cubic) for different choices of  $\alpha$ , respectively. Gray solid, dashed, and dotted gray curves show MB, UM, and  $r$ -concave stability selection with  $\tau = 0.75$ . The dashed black line represents perfect E(FP) control.

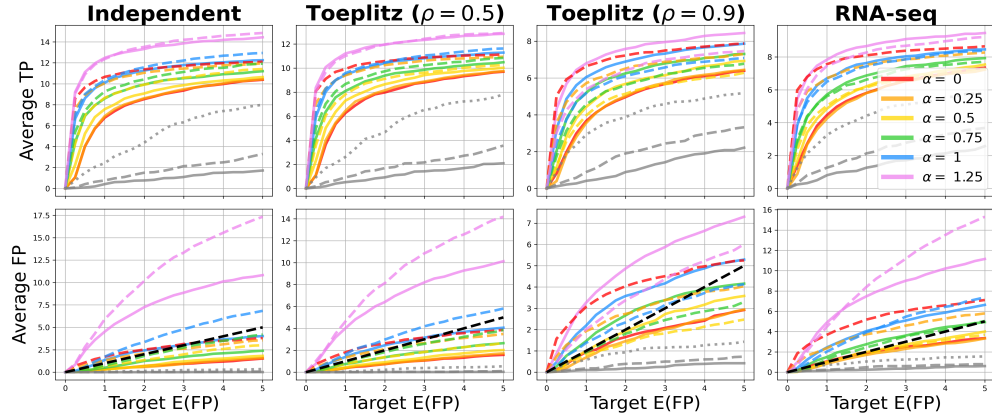


FIGURE S21. *Sensitivity to  $\alpha$ : Lasso, ( $p = 1000$ )*. See Figure S20.

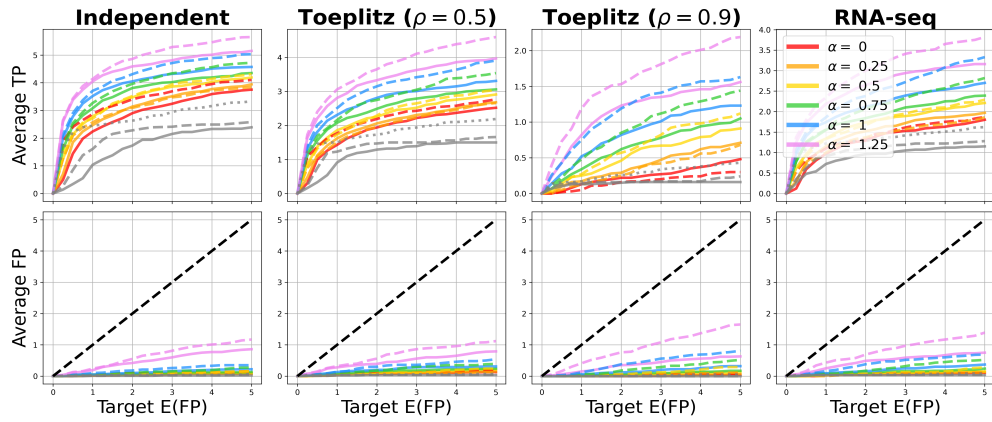


FIGURE S22. *Sensitivity to  $\alpha$ : MCP ( $p = 200$ )*. See Figure S20.

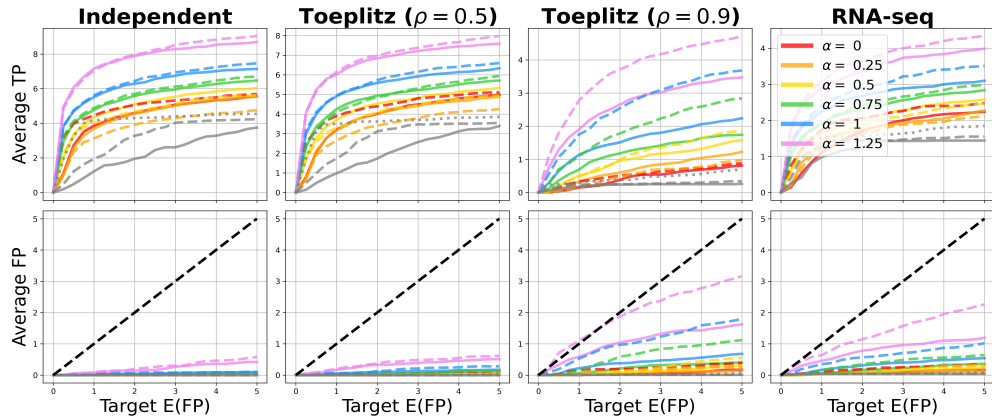


FIGURE S23. *Sensitivity to  $\alpha$ : MCP ( $p = 1000$ )*. See Figure S20.

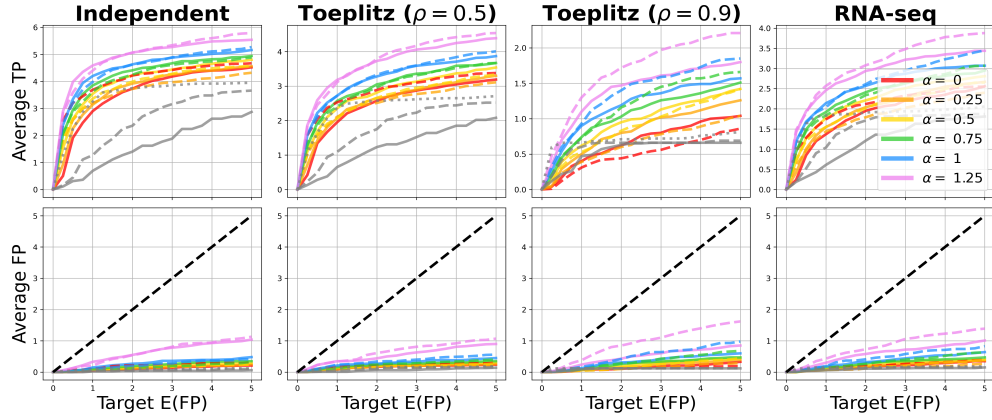


FIGURE S24. *Sensitivity to  $\alpha$ : SCAD ( $p = 200$ )*. See Figure S20.

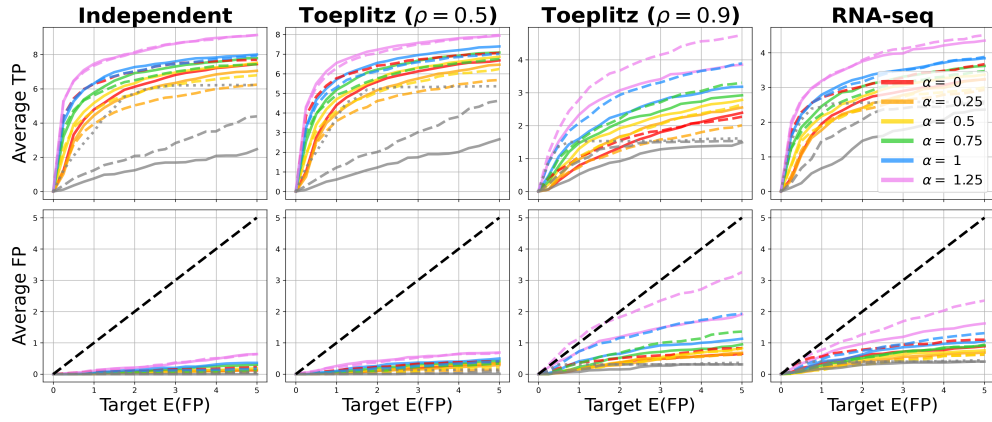


FIGURE S25. *Sensitivity to  $\alpha$ : SCAD ( $p = 1000$ )*. See Figure S20.

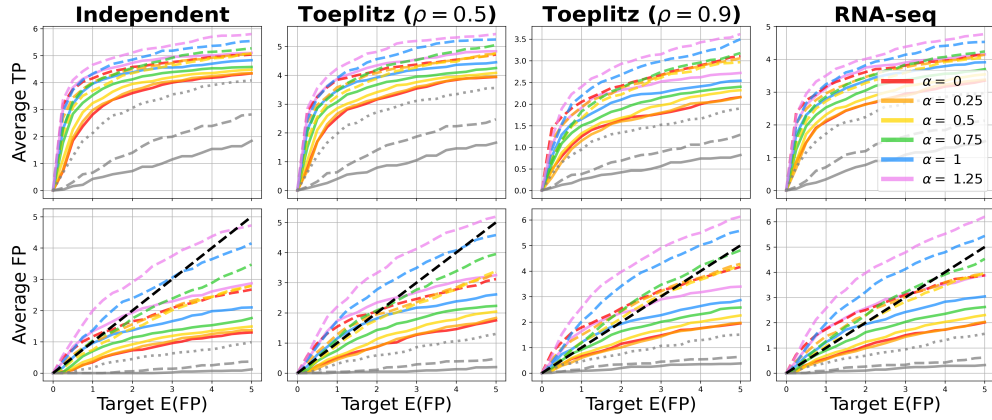


FIGURE S26. *Sensitivity to  $\alpha$ : Logistic regression ( $p = 200$ )*. See Figure S20.

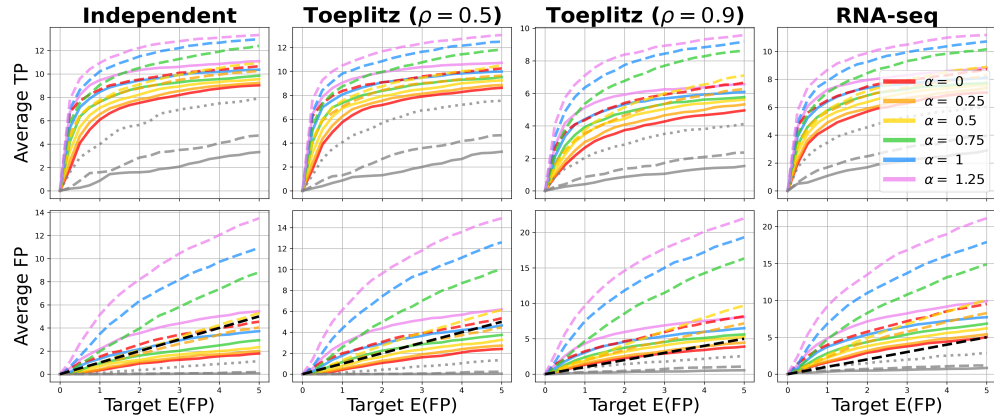


FIGURE S27. *Sensitivity to  $\alpha$ : Logistic regression ( $p = 1000$ )*. See Figure S20.